RADIO DIRECTION FINDING & SMART ANTENNAS

by

Murat Kebeli

B.S, Department of Electrical-Electronics Engineering, Boğaziçi University, 2007

Submitted to the Institute for Graduate Studies in
Science and Engineering in partial fulfillment of
the requirements for the degree of
Master of Science

Graduate Program in Electrical-Electronics Engineering
Boğaziçi University
2015

RADIO DIRECTION FINDING & SMART ANTENNAS

APPROVED BY:

Prof. Mehmet Akar   . . . .
(Thesis Supervisor)

Prof. Emin Anarım   . . . .

Prof. Fatih Alagöz   . . . .

DATE OF APPROVAL: 25.12.2015

ACKNOWLEDGEMENTS

ABSTRACT

RADIO DIRECTION FINDING & SMART ANTENNAS

In this thesis, Radio Direction Finding (DF) and Smart Antennas are studied. DF refers to the science of determining the location of radio transmission sources. A DF system uses the characteristics of the radio signal such as amplitude and phase at each antenna element to estimate the direction of arrival (DOA). In practice, three basic methods are preferred in DF systems; Watson Watt, Interferometer and High Resolution methods. This work focuses on the implementation of a novel DF system based on the interferometer method. However, an ambiguity problem occurs in estimating DOA when antenna aperture becomes larger than the half of the incident signal's wavelength. The dominant work in the first part of the thesis is resolving this ambiguity in interferometric DF systems. It is verified that the FFT based DF system performance is improved with the increasing antenna aperture and that the working frequency bandwidth of the system is also increased by using a single antenna array.

The second part of the thesis focuses on *Smart Antennas* that can dynamically adjust the beam-pointing direction of the antenna array by applying phase delays to the antenna elements. There is a tremendous need and increase in use of smart antennas with the growth of mobile networks. Three basic beamforming approaches are used in smart antennas: fixed, switched and adaptive. We propose a novel multi-model beamforming model that integrates the switched and adaptive beamforming systems that combines the advantages of a switched and an adaptive beamforming systems. It gives faster response than an adaptive only system and provides perfect tracking to all possible combinations of desired signal and unwanted signals compared to a switched beamforming only system.

ÖZET

TELSİZ VERİCİLERİN YÖN TESPİTİ & AKILLI ANTENLER

Bu tezde, radyo frekansında yön tespiti (DF) ve Akıllı Antenler konuları incelenmiştir. DF, radyo frekansındaki (RF) telsiz verici kaynakların konumunu tespit etme yöntemidir. DF sistemi, RF bir işaretin yönünü tespit etmek için, işaretin anten dizisindeki her bir antende oluşturduğu faz ve genlik gibi karakteristik özelliklerini kullanır. Pratikte, Watson Watt, interferometri ve yüksek çözünürlük olmak üzere üç temel DF yöntemi tercih edilir. Bu tezde yeni bir yaklaşımla çok kanallı interferometrik DF sistemi üzerinde çalışılmıştır. Önerilen sistemin avantajları, dezavantajları ve problemleri ele alınmıştır. Anten açıklığının artması ile sistem performansının da artması benzetimlerle gösterilmiştir. Anten açıklığının, gelen işaretinin dalga boyunun yarısını geçtiği durumlarda, sistem birden fazla açı için aynı faz farkı değerlerine sahip olmaktadır. İlk kısımda yapılan asıl iş, önerilen yöntem ile bu belirsizliğin önemli bir aralıkta ortadan kaldırılmış olmasıdır. Böylece, anten açıklığı arttırılabildiğinden sistem performansının da artması sağlanmış, bir DF sisteminin tek bir anten dizisi ile çok daha geniş bir bantta çalışması sağlanmıştır.

Tezde üzerinde durulan ikinci ana konu ise bir anten dizisindeki anten elemanlarına faz gecikmeleri ekleyerek hüzme yönünü belirleyen *Akıllı Anten* sistemleridir. Mobil haberleşmenin büyümesiyle akıllı antenlere olan ihtiyaç artmakta, akıllı antenlerin kullanımı hızla yaygınlaşmaktadır. Akıllı anten sistemi tasarımlarında sabit, anahtarlamalı ve adaptif olmak üzere üç temel hüzme-yönlendirme yaklaşımı olmakla birlikte bunların birbirleri üzerine artı ve eksileri vardır. Bu tezde, önerdiğimiz anahtarlamalı ve adaptif hüzme-yönlendirme metodlarını birleştiren çoklu adaptif yaklaşım modeli, anahtarlamalı ve adaptif yöntemlerin avantajlarını birleştirmektedir.

TABLE OF CONTENTS

LIST OF FIGURES

LIST OF TABLES

LIST OF ACRONYMS/ABBREVIATIONS

AC	Alternating Current
AOA	Angle of Arrival
COMINT	Communication Intelligence
COTS	Commercial off-the Shelf
CW	Continuous Wave
dB	Decibel
DC	Direct Current
DF	Direction Finding
DOA	Direction of Arrival
DSP	Digital Signal Processor
ELINT	Electronic Intelligence
EOB	Electronic Order of Battle
ESM	Electronic Support Measures
FFT	Fast Fourier Transform
FM	Frequency Modulation
FPGA	Field Programmable Gate Array
HF	High Frequency
Hz	Hertz
IF	Intermediate Frequency
LO	Local Oscillator
RF	Intermediate Frequency
LMS	Least Mean Squares
MHz	Mega Hertz
MUSIC	Multiple Signal Classification
MSE	Mean Square Error
MVDR	Minimum Variance Distortionless Response
PC	Personal Computer
PCI	Peripheral Component Interconnect

PXI	PCI Extension for Instrumentation
RDF	Radio Direction Finding
RF	Radio Frequency
RMS	Root Mean Square
SDR	Software Defined Radio
SOI	Signal of Interest
SIR	Signal to Interference Ratio
SMI	Sample Matrix Inversion
SNR	Signal to Noise Ratio
SNOI	Signal Not of Interest
SOI	Signal of Interest
UHF	Ultra High Frequency
VHF	Very High Frequency

1. INTRODUCTION

Direction Finding (DF) refers to the science of determining the location of radio transmission sources. In practice, DF compromises of the locating, tracking and distinguishing the different radio transmissions sources. DF and Radio Direction Finding (RDF) are usually used interchangeably [1].

Radio direction finding terminology began during the early years of the nineteenth century with the work performed by Hertz, Marconi and Zenneck on directive antennas [2]. First DF inventors took the idea of using the non-isotropic or directional antenna pattern to determine the direction of arrival of the incoming signal [3]. They noticed that when a directional antenna was rotated 360 degrees on the azimuthal plane, the peak amplitude of the incoming signal occurred at the angle of arrival. The first directive antenna was introduced by Stone in 1899 [4] and Brown proposed to rotate the directional antenna in 1902 [5]. The first experiments in this field were made by Marconi in 1906 [3].

Immediately after World War I, enormous developments were made in DF technology hand in hand with the great improvements in the general vacuum-tube based radio technology. In spite of the fact that these early DF systems were very simplistic with respect to today's DF technology, they nevertheless founded the fundamental structures of today's advanced DF systems. The methods used in the DF systems started by simply turning a directive antenna 360 degrees and have been developed using multiple-antenna array and complex computer algorithms over the last century to find the direction of arrival of incoming Radio Frequency (RF) signals [1, 2].

The first type of target location system depending on the RF signals was the Passive Radio Direction Finding. The needs of both world wars inspired major advances in direction finding technology. Until the end of the World War II, the direction finding was focussed on the HF (High Frequency) band, 0.5-30 MHz frequency range due to the fact that long range telecommunication could not be achieved in another way at
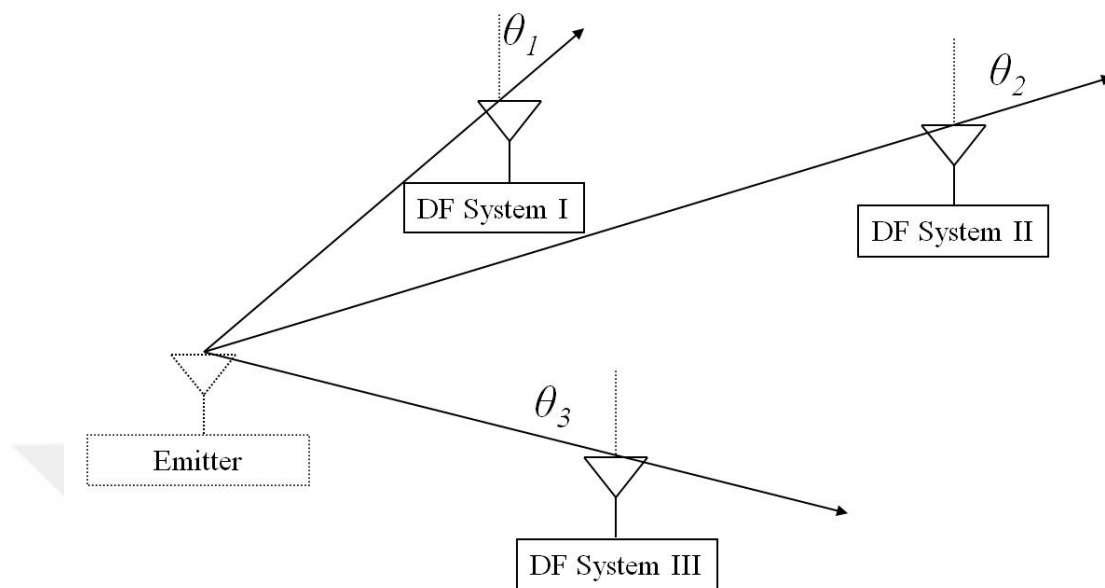
Figure 1.1. Triangulation by using 3 DF Systems

that time. Between World War I & II, very crucial developments in DF area were achieved. In addition, it is very interesting to note that the large majority of the patent protection was taken in this period [2].

Detection of not only the emitter direction but also the emitter location, requires 2 or more DF systems. These DF systems are located in different areas, all of which detect the direction of arrival of the interested electromagnetic signal at the same time. Angle of arrivals determined at all DF stations are collected at a central office and the location of the emitter of interest is detected by using these data. Figure 1.1 shows the detection of emitter location by using three DF systems. DF systems I, II and III try to resolve θ_1, θ_2 and θ_3, respectively. The locations of the DF systems are known and the location of the emitter is calculated at a central station. Since better estimation of direction of arrival is needed for a precise determination of the emitter location, the performance of each DF system is very important.

In order to obtain better estimates of direction of arrival, more sophisticated directional antennas were needed; therefore new methods had to be invented. Continuing

needs for better accuracy has been encouraging the researchers to improve the antennas for better performance in terms of more signal change per degree of angle of arrival and to create advanced DF methods and algorithms for better accuracy and resolution of the bearing angle [2].

1.1. Generation and Characteristics of Electromagnetic Waves

Charging and discharging routines on electrical conductors in the form of AC currents create electromagnetic waves. The length of the charging and discharging activity determines the wavelength of the electromagnetic wave. First of all, it is assumed that propagation of a harmonic wave of the wavelength (λ) is undisturbed. The radial field components of the electromagnetic wave decay rapidly with increasing distance. This simply allows us to assume that the electromagnetic wave in a small area is a plane wave. This further implies that, electric and magnetic fields are orthogonal and in-phase to each other and perpendicular to the radiation density vector that is defined as the direction of the propagation of the electromagnetic wave. The radiation density vector is defined as [6]

$$\overrightarrow{S} = \overrightarrow{E} \times \overrightarrow{H} = \overrightarrow{e}_0 \frac{|E|^2}{Z_0} \tag{1.1}$$

where $\overrightarrow{S}$ is the radiation density vector, $\overrightarrow{E}$ is the electric field vector, $\overrightarrow{H}$ is the magnetic field vector, E is the effective value of electric field strength, Z_0 is the characteristic impedance of free space $\cong 120\pi\ \Omega$ and e_0 is the permittivity of free space.

Direction of the propagation can be stated also by the wave number vector:

$$\overrightarrow{k} = \overrightarrow{e}_0 \frac{2\pi}{\lambda} \tag{1.2}$$

An electromagnetic wave behaves as a plane wave when the distance of the electromagnetic wave source from the receiving antenna system is greater than a specified length with respect to wavelength of the electromagnetic wave. This plane wave behaviour

simplifies the direction of arrival estimation for all DF methods.

1.2. Components of a Radio Direction Finding System

A DF system basically consists of the following subsystems:

- An Antenna Array
- DF Receivers (RF Receivers matched for DF)
- A DF Processor
- Display of the bearing angle

The antenna array is the front part of the DF system that receives the electromagnetic waves from the air. Radio Frequency (RF) signals should be lowered to an Intermediate Frequency (IF) to be processed by the DF processor. This crucial process is done by the DF processors. The most important difference of the DF receivers from classical receivers is the use of the same frequency synthesizer in all DF receivers for the phase and amplitude matched conversion from RF to IF. In order to decrease the calculation time of the angle of arrival, the number of receivers should be increased up to the number of antennas in the antenna array. On the other hand, increasing the number of DF receivers increases the power consumption proportionally and the cost of the hardware exponentially. By using an antenna array with two elements, the angle of arrival cannot be resolved due the same response of the antennas for $\theta°$ and $(\theta + 180)°$. By using three or more antenna elements, this ambiguity can be resolved [2,3].

1.3. Applications of Radio Direction Finding

DF systems are primarily used by military, civilian, government and research centers. Major application areas of DF systems are listed below:

- Air and marine navigation
- Search and rescue
- Frequency management

- Smart Antennas
- Communication intelligence (COMINT)
- Electronic order of battle (EOB)
- Electronic support measures (ESM)
- Emitter homing and locating
- Interference source location
- Emergency beacon location
- Spectrum monitoring
- Spectrum density calibrations

Direction finding systems can be also classified in three basic categories according to the aim of use [3]:

- Early Warning Threat Detection
- Targeting, Homing, and Jamming
- Electronic Intelligence

These are detailed below.

1.3.1. Early Warning Threat Detection

With the help of high-speed digital signal processing, it is possible to detect and identify a real threat in a dense radio frequency environment by using the status of the possible threat's amplitude, scan time, pulse width, period and modulation information. As a result, probable attacks can be recognized and necessary countermeasures can be taken without a delay [2].

1.3.2. Targeting, Homing, and Jamming

In today's military technology, missiles are launched in the general direction of the threat. An advanced radar system determines the target location and provides

the related guidance information to the missile. The missile's self radar starts to trace the threat as soon as the threat is in the range of the missile's radar. However, radio frequency radiation of the missiles radar can provide information about the missiles' position to the enemy. Missiles can use the passive direction finding system to detect the position of the threat without radiating any radio frequency energy [2].

Homing is also an important application area of the passive direction finding system. Homing is generally used by telecommunication authorities who control the frequency allocation plan of a country. Many interference radio frequency signals appear in the radio frequency bands that are booked. They disturb the other users and may cause serious problems in communication. Telecommunication authorities have to locate and eliminate these interferer RF emitters. In this sense, passive direction finding systems are indispensable for telecommunication authorities.

Repeater type jammers use the signals coming from the enemy's radar, and imitate the echo signals that is reflected from the material which is illuminated by radar signals. In this way, these jammers deceive the radars. However, in order to locate the radar without any radiation, these jammers have to be supported with a DF system that has a high angular resolution. Lens-fed and switched-phaseshift arrays are formed with the technological developments in this area to provide high angular resolution [2].

1.3.3. Electronic Intelligence

Electronic Intelligence (ELINT) refers to detecting new RF signals in the environment, differences of the locations of the threats/forces and controlling the radio spectrum and radar traffic in peacetime. In wartime, it is the basic system to determine the Electronic Order of Battle (EOB).

Radar is an active system; as such it cannot hide itself. RF frequency, pulse width, pulse interval are the basic descriptors of a radar. These descriptors are determined by an ELINT system and the type of the radar is detected by correlating with the collected data for different types of radars.

Passive radio direction finding is a counter-measure to active radars and other RF signals without giving away any information on the presence of the DF receiver's and operating technique. This is the reason why there is a relatively lack of published theory and information about the direction finding system. However, it has a vital role in locating the threats, radars and any other RF sources. This makes it indispensable for ELINT systems [2].

1.4. Motivation of the Thesis

Radio direction finding terminology began during the early years of the nineteenth century with the first directive antenna that was proposed by Stone in 1899 [4]. Then, Brown proposed to rotate this directional antenna in 1902 to find the direction of the incoming wave [5]. Right after Brown approach to direction finding of RF signal, Marconi made the first experiments of a DF system 1906 [3]. Both World Wars encouraged researches in this area and tremendous improvements were achieved during the World Wars. Watson Watt and Interferometer methods were defined before 1960s. Since early 1980s, high resolution DF methods have become more popular. The popularity of high resolution methods over classical methods (Watson Watt and interferometer) for researchers are still valid due to saturation of classical methods. However, in practice, the interferometer method has an overwhelming use compared to Watson Watt and high resolution methods due to its advantages over other methods. The advantage of the interferometer method over Watson Watt is that, interferometer gives much more accurate results than the Watson Watt method. On the other hand, in spite of the fact that high resolution methods gives a little bit more accurate results than interferometer, due the narrowband structure of these systems, interferometer based DF systems are preferred by users (military, government etc.) for its wide bandwidth and capability of finding directions of different signals at different frequencies (signals should be in the bandwidth of DF system) at the same time.

Interferometer DF systems have been investigated in all aspects over fifty years; therefore it is an settled method. The performance of this method increases with the increasing antenna apertures; nevertheless the apertures between antenna elements in

the antenna array should be lower than the half wavelength of the incident signal's wavelength. In addition, for a wideband DF system antenna apertures should be lower than half of the highest frequency's wavelength. For a DF system that has to cover all VHF and UHF band (30 MHz to 3000 MHz), antenna apertures differ from 0.5 λ to 0.005 λ. In this case, the DF system works well near the end of the UHF band and the performance of the system decreases with the decrease of the incoming signal's frequency. To solve this problem, more antenna array layers are used. For the system discussed above, approximately 0.1 λ to 0.5 λ can be achieved with three antenna array layers.

As mentioned above, the performance of interferometer based DF systems increases by increasing the antenna aperture up to the half wavelength of the DF system's highest input frequency not to be faced with AOA ambiguity. To achieve higher accuracy, non-symmetric antenna arrays have been proposed [3]. Thus, ambiguity is resolved by one or two antenna pairs providing smaller antenna aperture than half wavelength of the incoming signal; other antenna pairs may have higher apertures. However, for a wideband operation, all antenna pairs have to be different apertures and all pairs cannot be used for all frequencies. Handling mutual coupling problems also becomes more difficult.

Another research area on radio direction finding is *Smart Antennas*. As the demand for data communication increases, so does the required total bandwidth. Since the total frequency band is limited, radio frequency band should be used effectively. Smart antennas optimize the radio frequency band and provide multiple users who are in different directions to use the same radio band [40]. Smart Antennas improve efficiency by utilizing beamforming techniques. Switched and Adaptive Beamforming methods are widely used in Smart Antennas.

This thesis focuses on 2 different problems in RDF and Smart Antennas. The first one is to solve the ambiguity problem in RDF when all antenna apertures are higher than the half wavelength of the incoming signal. Non-symmetric antenna arrays can provide some antenna pairs that have apertures higher than the half wavelength

of the incoming signal but we strive to achieve this result for all apertures. Thus, more accurate results are obtained with symmetric antenna arrays compared to non-symmetric arrays due to more antenna pairs with higher apertures. In addition, this also provides using interferometer DF system with antenna arrays that have antenna apertures higher than the half wavelength of the incoming signal.

The second aim of the thesis is to provide a more efficient beamforming method for Smart Antennas. Three different approaches of the beamforming methodology are *fixed, switched and adaptive.* The fixed beamforming approach achieves the expected gain in the direction of the desired signal and side-lobe cancellation in the directions of the unwanted signals. However, it cannot be used in a variable electromagnetic environment. A switched beamforming system switches between the predefined beams and therefore can handle the signals in all directions. It uses fixed beamforming methodology in creating multiple predefined beams. Switched beamforming systems have very fast response to the changes in the direction of the target signals. On the other hand, they can not provide the optimum solution for every combination of desired and unwanted signals due to the limitation of number of the predefined beams. In addition, if the directions of the signals change with time, it cannot adopt itself to new directions. Adaptive beamforming methods are used to solve the problem with the signals that are changing the directions continuously. Adaptive beamforming systems have a feedback network and try to adopt themselves to new conditions in the electromagnetic environment. We propose a new model inspired from [7,8] that integrates the switched and adaptive beamforming systems. The proposed multi-model adaptive beamforming method combines the advantages of switched and adaptive beamforming systems.

1.5. Organization of the Thesis

In Chapter 2, basic direction finding algorithms are discussed. In amplitude comparison DF methods section, Watson Watt method is introduced; Doppler, Pseudo Doppler and Interferometer methods are introduced in phase comparison DF methods section. Classical Beamforming, Capon's Beamformer and MUSIC methods are investigated among high resolution DF methods section. The advantages and disadvantages

of all methods are also discussed.

In Chapter 3, Multi-Channel Interferometer methods such as Conventional Interferometer, Fourier Transform Method and Correlative Interferometer Method are discussed in detail. We also propose a hardware implementation for interferometer methods with a Software Defined Radio (SDR) environment. We investigate the effect of antenna apertures on DF accuracy for FFT based Correlative Interferometer method. We also examine our preferred method for solving the ambiguity problem for antenna apertures larger than the half wavelength of signal of interest (SOI).

Three basic beamforming approaches are used in smart antennas: *fixed, switched and adaptive beamforming*. These beamforming methods are reviewed in detail in Chapter 4.

In Chapter 5, we propose a new approach based on [7, 8] that integrates the switched and adaptive beamforming systems. The proposed multi-model adaptive beamforming method combines the advantages of switched and adaptive beamforming systems. The cons and pros of the proposed models against classical models are evaluated via simulation results.

Finally, concluding remarks are given in Chapter 6.

2. BASIC RADIO DIRECTION FINDING METHODS

2.1. Overview of Radio Direction Finding Methods

DF methods can be categorized into three basic classes:

- Phase comparison based DF methods
- Amplitude comparison based DF methods
- High Resolution DF Methods

In phase comparison based DF methods, minimum three antennas are located in such a manner that each angle of arrival of the incident wave creates unique phase differences between antennas. By using these phase differences, direction of arrival of the incident wave is estimated. Examples of such systems include Doppler DF methods and interferometer based DF methods [9–11].

In amplitude comparison based DF systems, minimum three antennas are located in such a manner that each angle of arrival of the incident wave creates unique amplitude differences between antennas. By appropriately analysing these amplitudes, direction of arrival of the incident wave is calculated [12]. Watson-Watt DF method is the most commonly used one among the amplitude comparison based DF methods. Wullenweber DF method is also in the category of amplitude comparison based DF systems [9].

With the advance of DF technology, high resolution methods like Capon's Beamformer and MUSIC (Multiple Signal Classification) have been introduced [13]. This group of methods has an advantage of finding the direction of more than one signals in the same frequency at the expense of narrower bandwidth.

2.2. Amplitude Comparison Based DF

Watson Watt and Wullenweber DF methods fall in this group. Due to its widespread use, the Watson Watt method will be discussed in detail below.

2.2.1. Watson-Watt Method

Watson-Watt DF is the most commonly used method in the amplitude comparison DF category. Generally, Adcock or loop antennas are used to form a Watson-Watt DF system. While loop antennas are preferred in lower frequencies due to their compact sizes, Adcock antennas are preferred in higher frequencies due to their superior performance. Antennas are placed to create a figure-of-eight azimuthal gain pattern by the difference of the reciprocal antennas' voltages. Figure 2.1 shows the azimuthal gain patterns of an Adcock DF antenna used for the implementation of Watson Watt method [14, 15]. Referring to Figure 2.1, we vectorially subtract the N and S antenna elements' voltages to produce the "Y-axis" voltage and we vectorially subtract the E and W antenna elements' voltages to produce the "X-axis" voltage. The AOA is estimated by using these measurements.

Watson Watt DF systems are the ancestors of all DF systems. Due to their small antenna array size compared to other methods, they are still preferred especially for mobile applications. However, in tactical applications, other methods are used due to their superior performance over Watson Watt.

2.3. Phase Comparison DF Methods

Doppler and interferometer RDF methods fall in this group. These methods are detailed in this section.
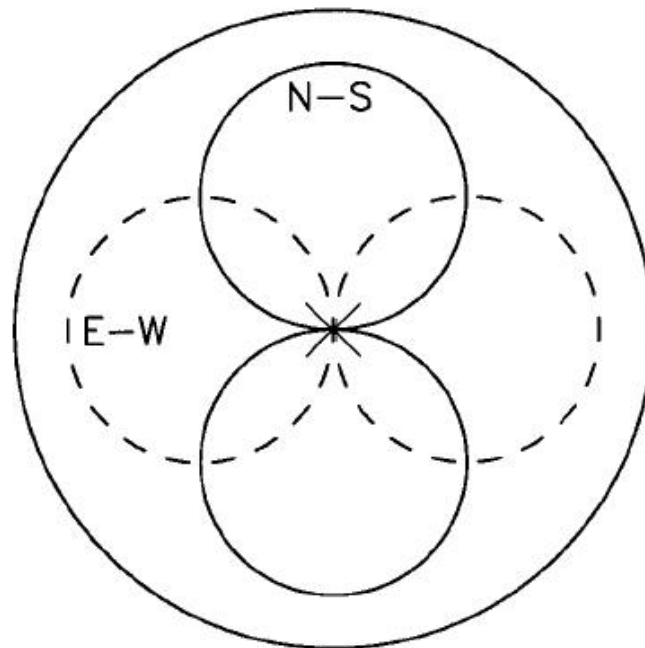
Figure 2.1. Azimuthal Gain Patterns of Adcock DF Antenna used for Watson Watt Method

2.3.1. Doppler Method

The concept of the Doppler DF system is inspired from the "Doppler effect" which is defined by the Austrian physicist Christian Doppler in 1842. Doppler effect is the change in the frequency of a wave coming from a moving source relative to an observer, so it is directly proportional to the relative speed of the source and the receiver. If the moving source is getting closer, the relative frequency of the wave becomes higher; in the same way, as the moving source is moving away, the relative frequency of the wave becomes lower. To give an example, the siren of an approaching ambulance is heard by the observer with a fixed pitch higher than its actual stationary pitch, as the ambulance passes near the observer. As it goes further away, the pitch frequency of the heard by the observer suddenly becomes a new fixed frequency pitch that is lower than the actual stationary pitch. The lower and the pitch frequencies heard by the observer are fixed because the ambulance approaches to the observer and goes far away from the observer at a fixed speed.

Doppler effect for radio frequency signals can be observed as the RF transmitter approaches to the RF receiver, the frequency seen by the receiver side becomes higher than the actual frequency transmitted by the transmitter. As the RF transmitter goes further away from the RF receiver, the frequency seen by the receiver side becomes lower than the actual frequency transmitted by the transmitter. Thus, the frequency appearing at the receiver side is dependent to the relative movements of the receiver and the transmitter.

By employing the Doppler effect phenomenon in Direction Finding, Earp and Godfrey of Standard Telephones and Cables Ltd was the first to formally introduce the Doppler DF system in 1947 [16]. The first Doppler DF systems made use of the Doppler Effect by using a turntable and an antenna on it. The turntable is rotated at a constant high speed. As the antenna approaches to the incident signal source, the frequency received by the antenna increases. In a similar manner, as the antenna moves in a reverse direction to the incident signal source, the frequency received by the antenna decreases. The output of the antenna has a frequency modulated tone at the frequency of the rotation. The output of the antenna is connected to an FM demodulator whose output will be the same tone with the rotational frequency. The only difference is the phase differences of the tones. This phase difference is used to determine the angle of arrival [16, 17].
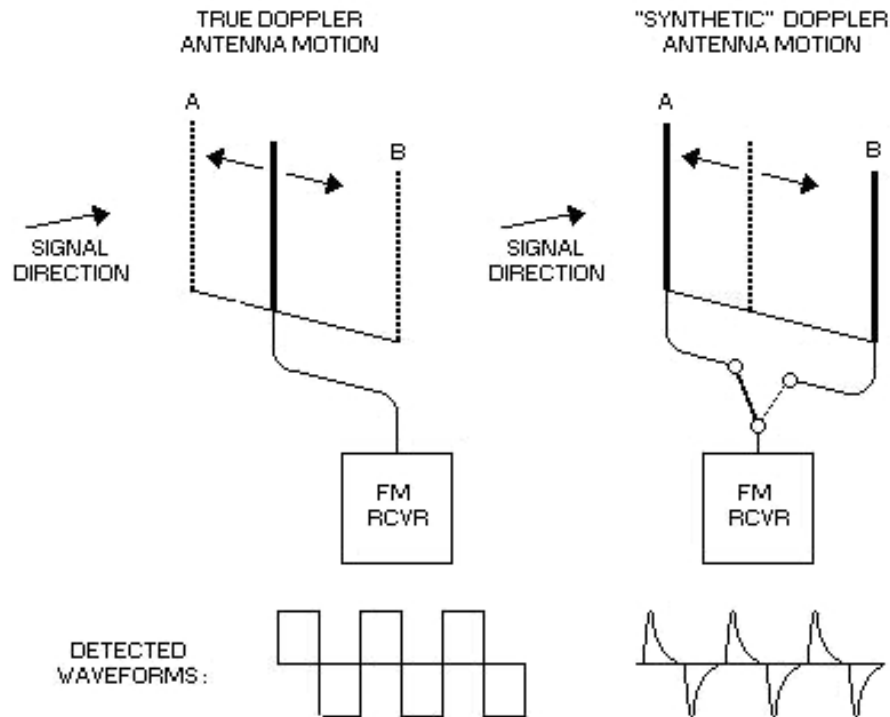
Figure 2.2. Doppler Shift Produced With the Moving Antenna and Switching Antenna [18].

Figure 2.2 shows the Doppler shifts that are created by the phase differences between the two antenna signals. Antenna "B" is farther to the RF transmitter than antenna "A". The signal comes to antenna "B" with a time delay compared to antenna "A", since the signal has to be travel more to arrive at antenna "B", which induces a phase delay occurring to the signal at antenna "B" compared to the signal at antenna "A". This phase delay is directly proportional to the incident wave's angle of arrival (AOA). It is maximum if the direction of arrival of the incident wave is parallel to the A-B line, and is zero if the direction of arrival of the incident wave is orthogonal to the A-B line. To give an example, if the incident wave has to be travel 1/6 wavelength more to reach antenna "B", the phase delay between antennas will be 360/6=60 degrees [18].

2.3.2. Pseudo-Doppler Method

The Pseudo-Doppler DF method is accepted as the single channel interferometer DF method due to its dependence on the phase differences between 3 or more antennas. Pseudo-Doppler DF systems are the technologically elegant versions of the classical Doppler systems. They have some important advantages over true Doppler systems such as eliminating mechanical difficulties and effects of rotating antenna due to its simple design and implementation. All of the modern Doppler DF systems are Pseudo-Doppler DF systems and true Doppler DF systems are rarely or not used in today's direction finding applications.

The Pseudo-Doppler direction finding method is actually a phase comparison DF method that depends on the phase differences of the antenna elements which are circularly disposed. As mentioned in Section 2.3.1, the frequency shift caused by the Doppler effect can be determined by rotating an antenna mechanically and then, the direction of arrival can be calculated by using this frequency shift. Due to difficulties of rotating an antenna with a known and fixed speed, the Pseudo-Doppler DF method has been developed. In this method, the Doppler Frequency shift is created by switching the receiver antenna of the antenna array which are equally and circularly disposed (Equally and circularly disposition of the antennas is for easy implementation of the Pseudo-Doppler method). Frequency of the incoming wave signal suddenly changes at the switching instants. This frequency shift is actually the phase differences between the antennas. The output of the switching circuitry feeds an FM demodulator. By using the information gained from the FM demodulator output, phase differences between adjacent antennas can be determined and used to determine the incident wave's direction of arrival [19].
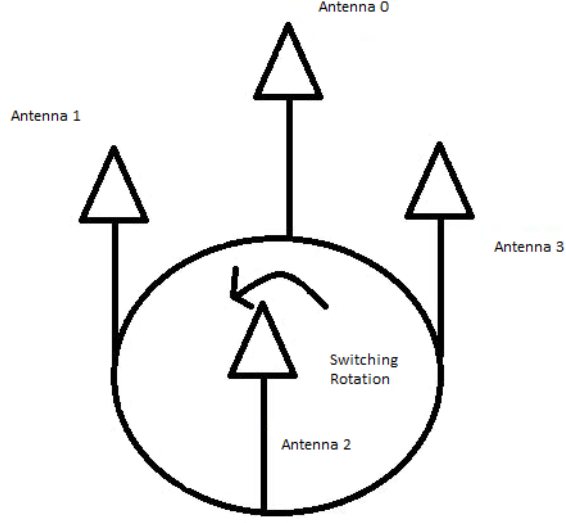
Figure 2.3. Four Element Antenna Array for Pseudo Doppler DF System.

For a deeper explanation of a Pseudo Doppler DF system, consider the antenna array depicted in Figure 2.3, where the antenna array is symmetrically disposed as a circular array with an aperture of antennas lower than $\lambda/2$. For simplicity, suppose that all antennas have the same characteristics and there is no mutual coupling between each other. Assume that a signal source, at a position far enough to make an assumption that the wave behaves as a plane wave, creates a continuous wave signal at frequency that has a wavelength greater than twice the distance between adjacent antennas. The signal received at each antenna element will have a phase shift from its neighbour antennas. The amount of the phase shift depends on the AOA of the incident wave, the frequency and the antenna positions. The signal created at each antenna i is given by

$$S(t, i) = I(t) X_i \qquad (2.1)$$

where the i-th element response X_i is

$$X_i = e^{j \frac{2\pi r}{\lambda} \cos\left(-\frac{2\pi i}{N} + \Phi_{AOA}\right)} = e^{\theta_i(\Phi_{AOA})} \qquad (2.2)$$

Here, $I(t)$ is the received RF signal at the center of the array, r is the array radius in meters, λ is the wavelength of the RF signal in meters, N is the number of elements in the array, Φ_{AOA} is the angle of arrival in radians referenced clockwise from antenna 0, and i is the antenna index. Antenna elements are commutated in the counter-clockwise (or clockwise) direction, from antenna 0 to 1 and so on. An FM demodulator is fed by the commutation switch's output. The FM demodulator output will have impulses at switching instants that are proportional to the phase shifts. Then, a narrowband band-pass filter with a center frequency equals to switching rate is used. The output of the filter will be a sine wave. The phase of the sine wave output at the switching instant from antenna 0 to 1 is used to calculate the angle of arrival [20].

2.3.3. Interferometer Method

In the literature, interferometer and phase interferometer methods refer to the same method. The interferometer method relies on the phases of the incident wave signal at different antennas. Since the Pseudo Doppler method also depends on the phases of the received signal at distinct antennas, the Pseudo Doppler method is also accepted as single channel implementation of the interferometer method. Basically, an antenna array consisting of three or more antennas that are disposed in the horizontal in an appropriate manner is used as the antenna system of an interferometer Direction Finding System. The outputs of these antennas are connected to phase coherent identical receiver system. The phase coherency of the receivers may be the most important point in implementing a phase dependent DF system. This receiver system takes RF signals from antennas and converts them to a lower Intermediate Frequency (IF) for ease of processing. The outputs of the phase coherent receiver systems are fed to the DF processor that first determines the phase differences between the signals and then calculates the angle of arrival of the incident wave signal. The interferometer methods will be discussed in more detail in Chapter 3.

2.4. High Resolution DF Methods

High Resolution Methods can determine the DOA of signals at the same frequency while classical techniques cannot. Since these algorithms use the data taken from an antenna array, they are classified as Array Processing techniques. Classical Beamforming, MUSIC (MUltiple Signal Classification) and Capon's Beamformer are the well known examples of high resolution direction finding methods.

2.4.1. Classical Beamforming

This method depends on measuring the power of the incident wave at each angle of arrival. The direction of arrival estimation is done by selecting the angle of arrival where the maximum power is achieved. The power measurement at each angle of arrival is carried out by forming a beam in each angle and setting the beamformer weights equal to the corresponding steering vector at the same angle [13, 21, 22].

The array output of a beamforming system is given by:

$$y[n] = \sum_{k=1}^{N} w_k x_k[n] \tag{2.3}$$

where $x_k[n]$ is the received signal at instant n, w_k is the weighting vector of the beamformer, N is the number of antenna elements in the antenna array. By setting $w = [w_1, w_2, ... w_n]^T$, $x_n = [x_1[n], x_2[n], ... x_N[n]]^T$, (2.3) can be represented as

$$y[n] = w^H x_n \tag{2.4}$$

Thus, the power at each angle of arrival can be calculated by:

$$P(\theta) = E\left[|w^H x_n|^2\right] \tag{2.5}$$

$P(\theta)$ will have maximas at the angles where the corresponding steering vectors are equal to the beamformer weights. DOA resolution can be increased only by increasing the number of antennas in the antenna array. The main problem here is that the weighting vector has large side-lobes. Although the main lobe has narrow width, the large side-lobes cause more power to enter in different angle of arrivals and decreases the resolution of DOA estimation.
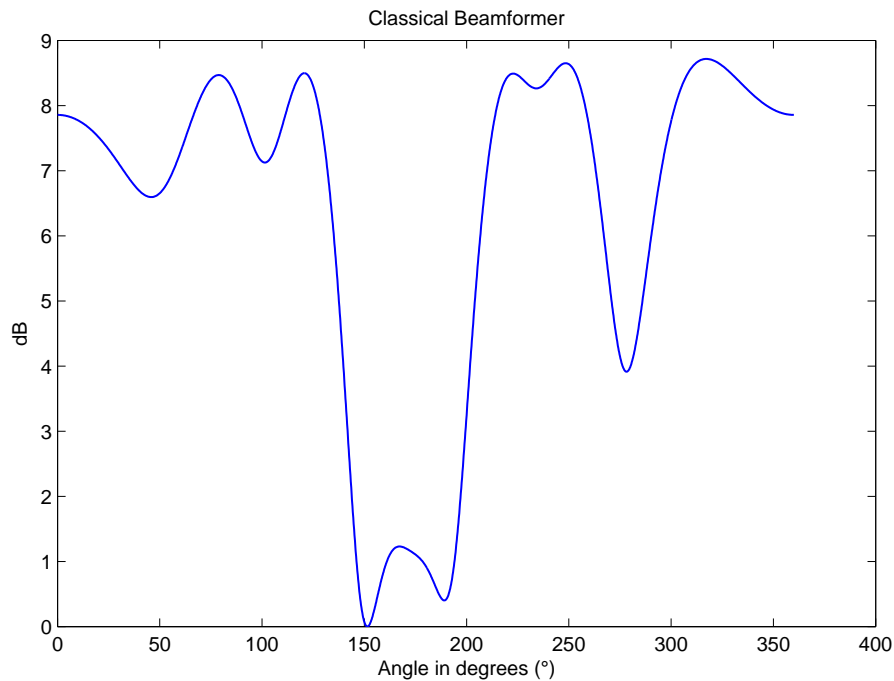
Figure 2.4. DF function of Classical Beamformer ($S/N = 5$); wave angles: 80°, 120°, 220°, 250°, 320°.

Figure 2.4 shows the DOA estimation of Classical Beamforming method for the incident waves coming from angles 80°, 120°, 220°, 250°, 320°'s with an $S/N = 5$.

2.4.2. Capon's Beamformer

Capon's beamformer method, also known as Minimum Variance Distortionless Response Method, was proposed by J. Capon in 1969 [24]. This method is very similar to the Classical Beamformer method. It relies on measuring the power of the incident

wave at each possible angle of arrival, which is done by setting the beamform gain to 1 in that direction, in order to minimize the output power from signals that are coming from other directions. Actually, this is a constrained minimization process. The signal power

$$\min_{w} E\left[|y\left(k\right)|^2\right] = \min_{w} w^H R w \qquad (2.6)$$

is minimized with respect to weighting vectors subject to $w^h a\left(\theta\right) = 1$, where w is the weighting vector, R is the cross correlation matrix of the input signals, and $a\left(\theta\right)$ is the steering vector for angle θ. The maximas at the angles stand for the angle of arrival estimations of the method. MVDR beamformer is defined in [24] by Capon as the solution of this optimization problem and its weights are given by:

$$w = \frac{R^{-1} a\left(\theta\right)}{a\left(\theta\right) R^{-1} a\left(\theta\right)} \qquad (2.7)$$

The advantage of this method over Classical Beamforming is its higher AOA resolution at the expense of an inverse matrix computation that may become problematic with correlated input signals [13].

Figure 2.5 shows the comparison of classical beamforming and Capon's beamformer implementations for the incident waves coming from angles 80°, 120°, 220°, 250°, 320°s with an $S/N = 5$. As easily seen, the AOA resolution of Capon's method outperforms Classical Beamforming.

2.4.3. MUSIC

MUSIC (MUltiple SIgnal Classification) was proposed by Schmidt in [25]. MUSIC algorithm depends on separating the outputs of the antenna array into two subspaces: the signal subspace and the noise subspace. To do this separation, the method should have to estimate the noise subspace correctly. If the noise subspace is precisely estimated, it will be orthogonal to the signal subspace. In order to determine the steering
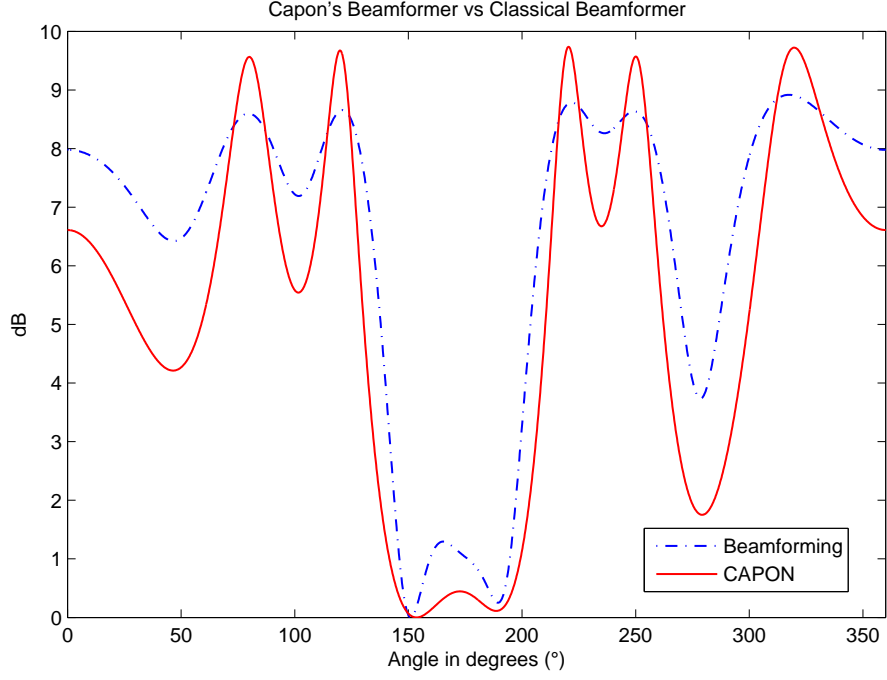
Figure 2.5. DF function of Capon's Beamformer vs Classical Beamformer ($S/N = 5$); wave angles: $80°$, $120°$, $220°$, $250°$, $320°$.

vectors orthogonal to the noise subspace, MUSIC proposes to search all possible steering vectors. For orthogonality, we have

$$a\left(\theta\right)^{H} Q_{n} = 0 \tag{2.8}$$

where $a\left(\theta\right)$ is the steering vector and Q_{n} is the noise subspace.

The errors in estimating the noise subspace causes $a\left(\theta\right)$ not to be precisely orthogonal to noise subspace. The function referred as the MUSIC spectrum is defined by Schmidt [25] as

$$P_{MUSIC} = \frac{1}{a\left(\theta\right)^{H} Q_{n} Q_{n}^{H} a\left(\theta\right)} \tag{2.9}$$

When θ is equal to the direction of arrival of one of the incoming signals, this function

results in very large values. Thus, DOA estimations of the incoming signals are made by using the MUSIC spectrum [13].
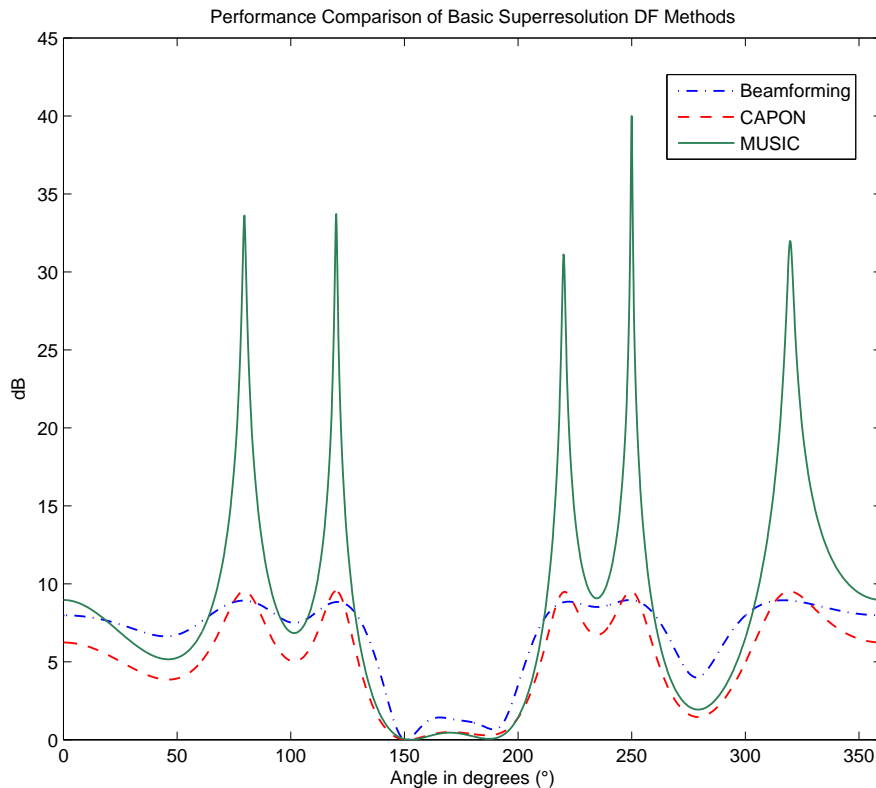
Figure 2.6. DF function of MUSIC vs Capon's Beamformer and Classical Beamformer ($S/N = 5$); wave angles: $80°$, $120°$, $220°$, $250°$, $320°$.

Figure 2.6 shows the comparison of classical beamforming, Capon's beamformer and MUSIC implementations. As easily seen, MUSIC has a superior performance over the other two methods. Correlated input signals are problematic also for MUSIC as in Capon's beamformer. Among many improvements to overcome this problem Root MUSIC is one of the most popular one [26]. Another problem in MUSIC is that, one should have to predefine the number of incoming signals. In practice, this is not possible. Several solution alternatives have been proposed for this problem [23, 27–29].

2.5. Summary of the Chapter & Concluding Remarks

In this chapter, we review the basic direction finding algorithms. First, we discuss the Watson Watt method in detail. DF systems that employ Watson Watt technique are still preferred especially for mobile applications due to their small antenna array size compared to other methods. However, in tactical applications, other methods are preferred because of their superior performance over Watson Watt.

On the other hand, the interferometer method that falls into the category of phase comparison DF methods has some advantages over other methods. The advantage of the interferometer method over Watson Watt is that, the interferometer gives much more accurate results than Watson Watt. In spite of the fact that high resolution methods provide a little bit more accurate results than the interferometer, due to the narrowband structure of these systems, interferometer based DF systems are preferred by users (military, government etc.) much more than high resolution DF systems for its wide bandwidth and capability of finding directions of different signals at different frequencies (signals should be in the bandwidth of DF system) at the same time. However, for better accuracy with interferometer method, antenna apertures should be increased over half wavelength of the SOI which causes an ambiguity problem. We will make suggestions to overcome this handicap in Chapter 3.

3. FFT BASED CORRELATIVE INTERFEROMETER METHOD

3.1. Multi-Channel Interferometers

The interferometer method relies on the phases of the incident wave signal at different antennas. Since the Pseudo Doppler method also utilizes the phases of the received signal at distinct antennas, the Pseudo Doppler method is also accepted as single channel implementation of the interferometer method. In this chapter, we will discuss multi-channel interferometer based RDF methods in detail.

Interferometer based DF systems have many advantages over other DF systems, including better accuracy, high bandwidth, and higher speeds. In addition, while all DF systems suffer from multi-path effects caused by the environmental conditions, like reflection off towers, buildings, power lines and other structures, the interferometer method minimizes these effects by using wide aperture antenna arrays [16]. As the antenna aperture increases over half of the incoming wave signal's wavelength, it causes ambiguity to determine the true direction of arrival that cannot be resolved easily [30]. One method to resolve this ambiguity is to use different antenna apertures in the antenna array so that at least one of the antenna apertures is always shorter than half of the incident wave's wavelength [31]. In this thesis, we propose an alternative method to eliminate this ambiguity.

3.1.1. Conventional Interferometer Techniques

The interferometer methods discussed above depend on the phase differences of two or more antennas. Figure 3.1 shows the geometry for two antennas with spacing d and incident waveform coming from the angle θ.

Incident wavefront received at antenna *1* travels an additional distance $(d \times \sin \theta)$
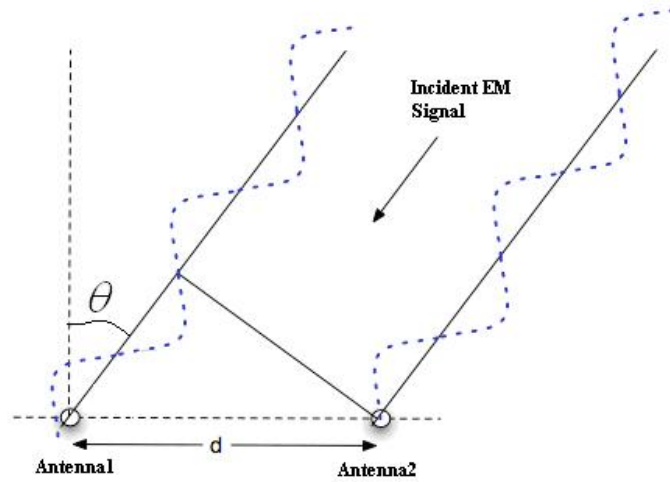
Figure 3.1. Phase Difference Between Two Antennas.

with respect to antenna *2*. The time to travel this distance between antenna *1* and antenna *2* creates a phase difference of $\Delta\Phi$ given by

$$\Delta\Phi = \frac{2\pi d}{\lambda}\sin\theta \qquad (3.1)$$

The angle of arrival θ can be calculated from (3.1) as

$$\theta = \arcsin\left[\frac{\Delta\Phi\lambda}{2\pi d}\right] \qquad (3.2)$$

where λ is the wavelength of the received signal and d is the distance between antennas. If only 2 antennas are used, for the angle of arrival of the incident waveform for $\theta°$ and $\theta + 180°$, the resulting AOA will be same. To determine the correct AOA, the system needs 3 or more antennas; this implies 2 or more baselines for the antennas.

Figure 3.2 shows the setup for the conventional phase difference detection method. The signals received by the antennas go into the phase comparator component, which correlates the signals and produces a DC output for the corresponding phase difference. Then, the output of the phase comparator is taken by the DF processor and the bearing
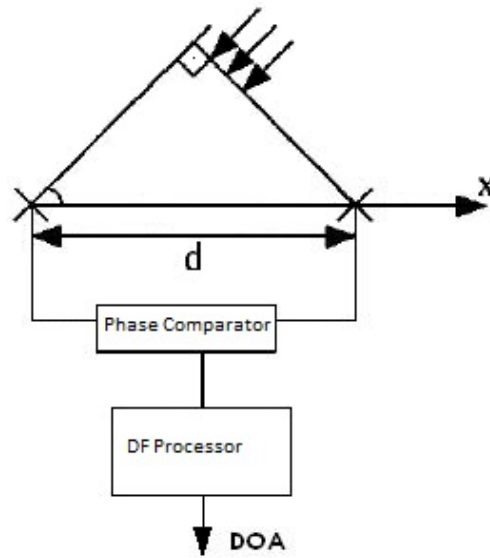
Figure 3.2. Phase Difference Detection.

angle is calculated.

3.1.2. Fourier Transform Method

Since interferometer methods rely only on the phase differences of the antennas of a DF system, different approaches have been used for measuring the phase difference between the antennas. With the important advances in the receiver and digitizer (Analog to Digital Conversion and Digital Downconversion) technology, the incident signals received by the antennas are digitized and then processed in digital world.

In order to measure the phase difference of the signals taken from different antennas, a phase coherent multi-channel RF receiver is needed. Common synthesized local oscillators are used for the downconversion of the signal from RF to IF for a phase coherent measurement. Analog to digital conversion is as important as matched-receivers for Fourier transform method. The outputs of the matched-receivers should be digitized always at the same sampling rate and at the same time, which requires digitizers having the same clock information.

After obtaining the digital data, Fast Fourier Transform (FFT) algorithms can be implemented easily to decrease computation time. FFT converts the time domain signal into frequency domain complex data. The transformed data contains frequency information at each point regarding its position. Each complex point in the frequency domain has real and imaginary components. The phase in the k-th frequency point is given by

$$\Phi_k = \arctan\left(\frac{i_k}{r_k}\right) \tag{3.3}$$

where r_k and i_k is the real and imaginary part of the k-th frequency point, respectively. The phase difference of the received signals from different antennas is

$$\Delta\Phi = \Phi_{i+1} - \Phi_i \tag{3.4}$$

where i is the antenna index. The phase difference information calculated from the signals of all antennas is used for calculating the AOA.

The FFT method has many important advantages over classical phase measurement methods (like using phase comparator etc.) such as [3]:

- Adverse effects of signal amplitude variations in measuring the phase differences are reduced substantially,
- Sensitivity of the spectral processing is improved more than 20 dB,
- Frequency dependent calibration and phase correction for all frequencies can be done easily. Phase errors can be easily eliminated for each frequency,
- FFT effective bandwidth is adjustable; therefore it is possible to determine the direction of arrival of the short duration signals. It improves the system's minimum signal duration for calculating the AOA,
- FFT output data can be saved and used to average more instants to improve the accuracy,
- The unwanted effects of interfering and jamming signals can be eliminated by the

opportunity of using adjustable resolution bandwidth.

All these advantages are achieved from the FFT method at the expense of high speed analog to digital conversion and high speed calculating performance by using developed FPGAs (Field Programmable Gate Array) and DSPs (Digital Signal Processor) [3].

3.1.3. Correlative Interferometer

Correlative interferometer is a method that is based on phase measurements. Any interferometer technique can be used to determine the phase differences of the antenna system. Correlative interferometer uses these phase differences to estimate the direction of arrival. An important advantage of the correlative interferometer is that it reduces the mutual coupling effects of the antennas while estimating the DOA. The steps of the correlative interferometer are as follows:

(i) Measure the phase differences of antenna system for the known directions and save all phase differences for all directions in a table. For example, make phase measurements for each 10° from 0° to 360° and save them in a lookup table.

(ii) Interpolate the lookup table for better resolution (like 1° or 0.1°) (Note that it is possible to make measurements with finer resolution at the expense of increased computational complexity).

(iii) Measure the phase differences for the unknown AOA.

(iv) Correlate the measured data with saved data.

(v) Maximum correlation occurs at the true DOA.

3.2. FFT Based Correlative Interferometer

As discussed in Chapter 3.1, the FFT method for phase calculation has numerous advantages over classical methods. In this thesis, we combine FFT with Correlative Interferometer method to create the FFT based Correlative Interferometer Method for improved accuracy.
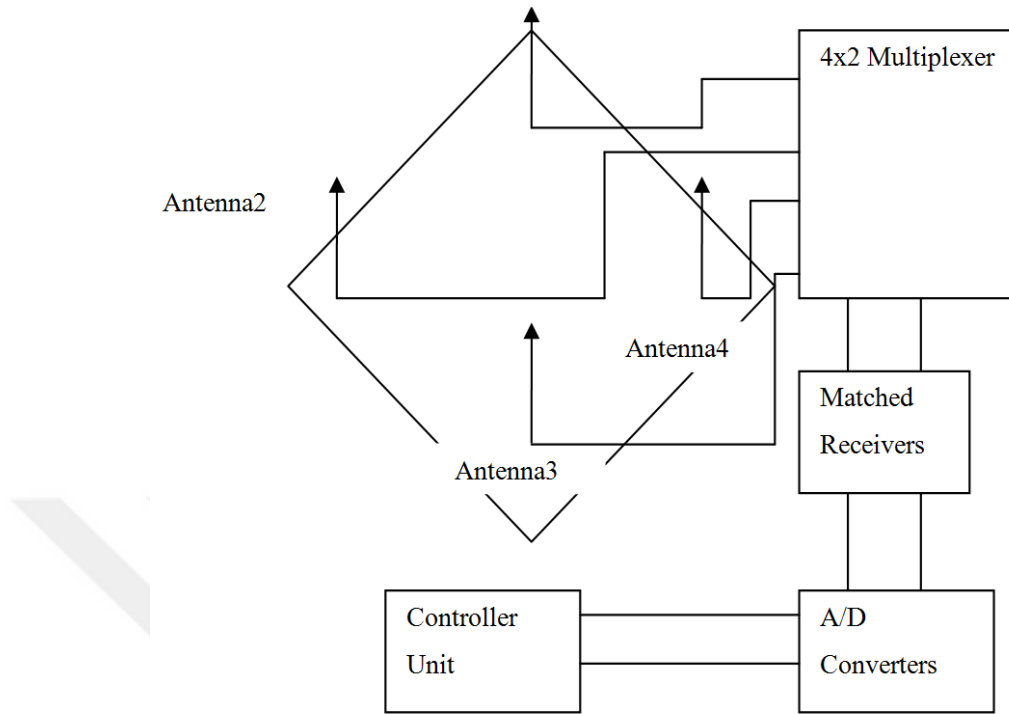
Figure 3.3. Schematic Diagram of the Software Defined Radio Use.

Figure 3.3 shows the block diagram of the Direction Finding System that is employed in this thesis. The system has n ($n = 4, 5, ..., 8$) antennas, each having the same distance to two of its nearest neighbours. The distance between antennas will be varied (e.g, d = $\lambda/4$, $\lambda/2$, λ and 2λ). For the simulations, phase differences of each two nearest antennas are calculated and a lookup table is formed. Then, the correlative interferometer method is implemented by using this lookup table. For simplicity, continuous wave (CW) signal at 500 MHz is used for calculations and simulations.

The interferometer methods discussed above depend on the phase differences of two or more antennas. Figure 3.1 shows the geometry for two antennas with spacing d and incident waveform coming from the angle θ.

Incident wavefront received at antenna 1 travels an additional distance $(d \times \sin\theta)$ with respect to antenna 2. The time to travel this distance between antenna 1 and antenna 2 creates a phase difference. Let us express the voltage received by antenna 2

as

$$V_2 = Ve^{jwt} \tag{3.5}$$

where V is the initial transmitted signal amplitude. Signal travels an additional distance $(d \times \sin \theta)$ to reach antenna 1, thus the voltage received by antenna 1 can be expressed as:

$$V_1 = Vexp \left(jwt + \frac{2\pi}{\lambda} dsin\theta \right) \tag{3.6}$$

where d equals to the antenna aperture and $\frac{2\pi}{\lambda}$ is the free space propagation constant. Subtracting V_2 from V_1 and taking to the natural logarithm of both side in order to obtain voltage differences between antennas yields:

$$ln V_2 - ln V_1 = ln\frac{V_2}{V_1} = jwt - jwt + \frac{2\pi}{\lambda} dsin(\theta) \tag{3.7}$$

$$= \frac{2\pi}{\lambda} dsin(\theta) \tag{3.8}$$

Initial transmitted signal amplitude V is used in both (3.5) and (3.6) so, it is eliminated in (3.7). Thus, it represents $\Delta\Phi$, phase differences between antenna 1 and antenna 2:

$$\Delta\Phi = \frac{2\pi}{\lambda} dsin(\theta) \tag{3.9}$$

Solving (3.9) for $sin(\theta)$ in terms of frequency by substituting $\lambda = c/f$ yields

$$sin(\theta) = \frac{30\Delta\Phi}{2\pi df} \tag{3.10}$$

where $\Delta\Phi$ is the phase difference in radians, f is the frequency of SOI in gigahertz, d

is the antenna aperture in centimeters, θ is the AOA. It can be expressed in degrees as

$$sin(\theta) = \frac{\Delta\Phi}{12df} \tag{3.11}$$

For an unambiguous AOA estimation, the phase shift $\Delta\Phi$ between antennas must be

$$0 < \Delta\Phi < 360 \tag{3.12}$$

The phase shift $\Delta\Phi$ repeats itself every 360 degrees for higher frequencies than the signals with a wavelength that equals to the twice of the antenna aperture d. This can be easily seen from (3.10) and (3.12). For the higher frequencies there will be more than one solution corresponding to the same $sin(\theta)$. This can be represented by

$$sin(\theta) = \frac{\Delta\Phi + 360M}{12df} \tag{3.13}$$

where M is the solution number and 360 comes from the repeating period of the phase shift. By rearranging the terms we obtain

$$\frac{d}{\lambda}sin(\theta) = \frac{\Delta\Phi}{360} + M \tag{3.14}$$

There will be no ambiguities until $d/\lambda = 1/2$. However, higher d/λ values will cause ambiguities, e.g, for $d/\lambda = 3$, change of AOA from $15°$ to $70°$ yields (3.14) result from 0.78 to 2.82. This implies 2.04 degrees of rotation and creates 2 ambiguities. It is impossible to solve these ambiguities for one baseline.

3.3. Simulation Setup

The received signal for each antenna element i is given by [20]

$$S(t, i) = I(t)X_i \tag{3.15}$$

where the i-th element response is:

$$X_i = e^{j\frac{2\pi r}{\lambda}\cos\left(-\frac{2\pi i}{N} + \Phi_{AOA}\right)} = e^{\theta_i(\Phi_{AOA})} \tag{3.16}$$

The phase of the incident wave X_i taken from the i-th antenna is calculated by using FFT. Then, phase differences between neighbour antennas are calculated by subtracting the phase of X_i from the phase of X_{i+1}. Figure 3.4 shows the calculated phase
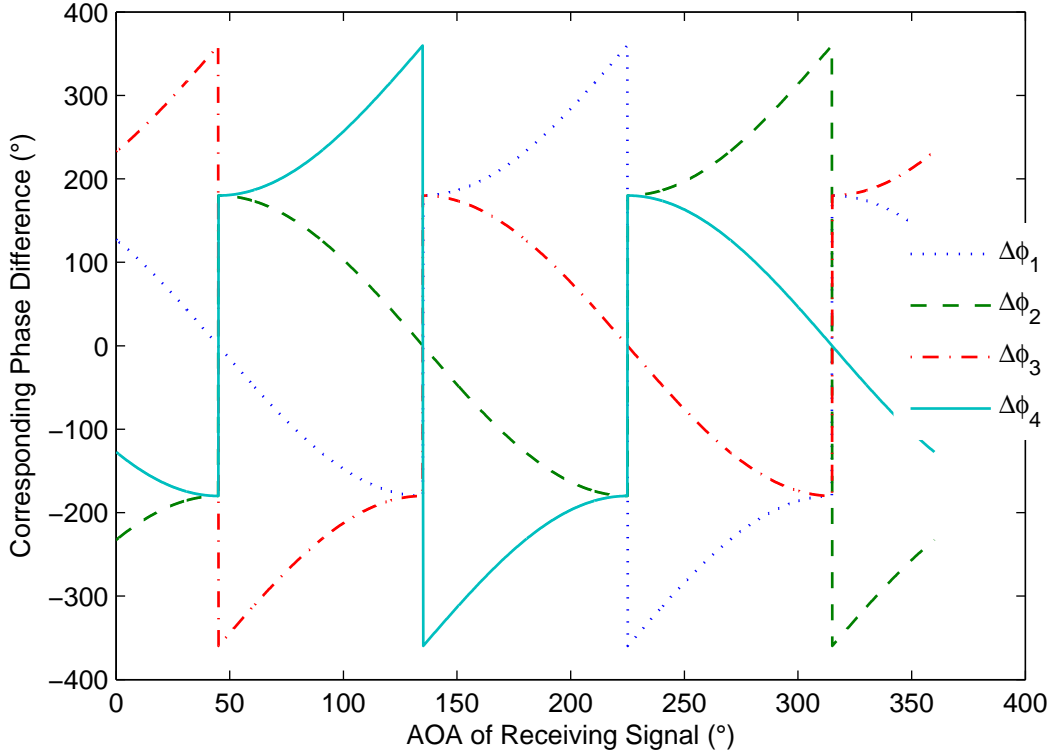
Figure 3.4. Calculated Phase Differences Between Antennas 2-1, 3-2, 4-3 and 1-4 for $d = \lambda/2$.

differences between each nearest neighbour antennas. Since the phase of the received signal of each independent antenna differs from -180°to 180°, the phase differences change between -360°to 360°. As easily seen in the figure, each phase difference has a different offset. This offset should be corrected to make the correct correlations. The phase differences should have to change linearly otherwise at the broken points of the phase difference, correlations will lead to big AOA estimation errors.
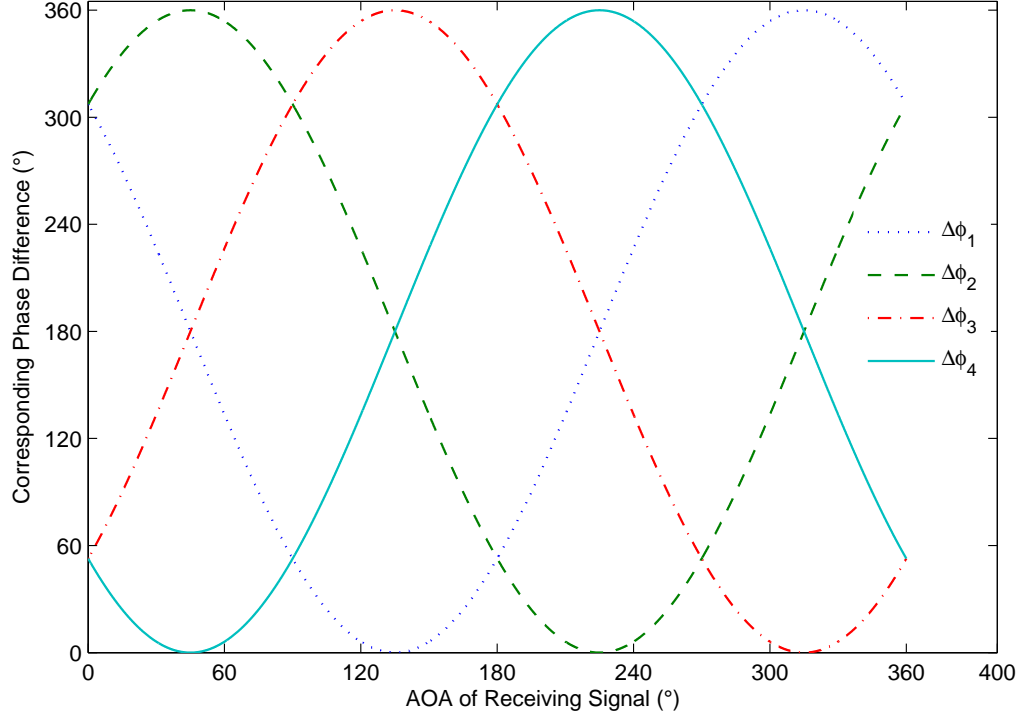
Figure 3.5. Calculated Phase Differences Between Antennas 2-1, 3-2, 4-3 and 1-4 for $d = \lambda/2$.

Figure 3.5 shows the calculated phase differences between antenna pairs 2-1, 3-2, 4-3 and 1-4 after adding proper offsets to prevent the phase ambiguities.

3.3.1. Euclidean Distance for Correlative Interferometer

We use Euclidean distances of measurement data to form the lookup table for the correlation method. The minimum Euclidean distance implies the maximum correlation. One can employ other distance measurement techniques, such as Manhattan and Minkowsky distances.
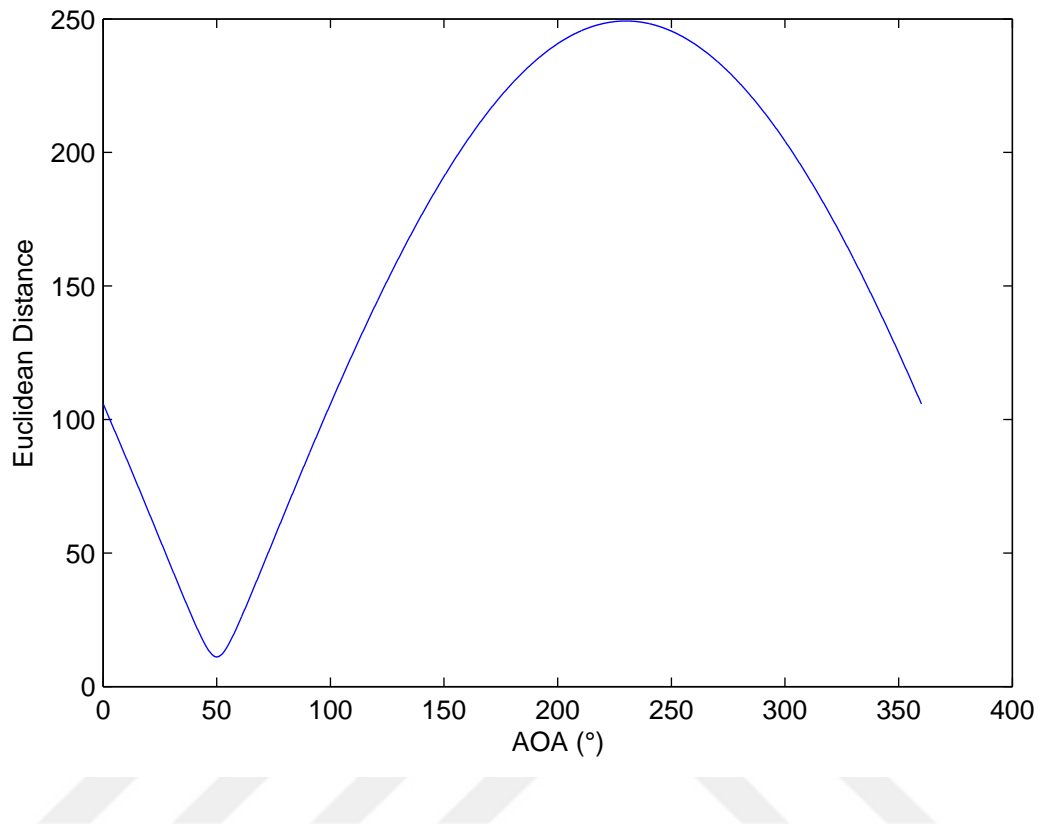
Figure 3.6. Euclidean distances of an AOA of 50° with "0" dB SNR.

Figure 3.6 shows Euclidean distances of measured data with an AOA of 50° with added noise to signal with "0" dB SNR.

3.3.2. Adding Noise to Signal of Intercept (SOI)

We add white Gaussian noise to the received signals. Figure 3.7 shows the measured phase differences between antennas 2-1, 3-2, 4-3 and 1-4 by adding noise at SNR = 0 dB. It is easily seen from the figure that the FFT method works well with the white Gaussian channel noise. Suppose we implement the correlative interferometer method by using a lookup table of 0.1° resolution to estimate the angle of arrival by using the calculated phase differences without noise.
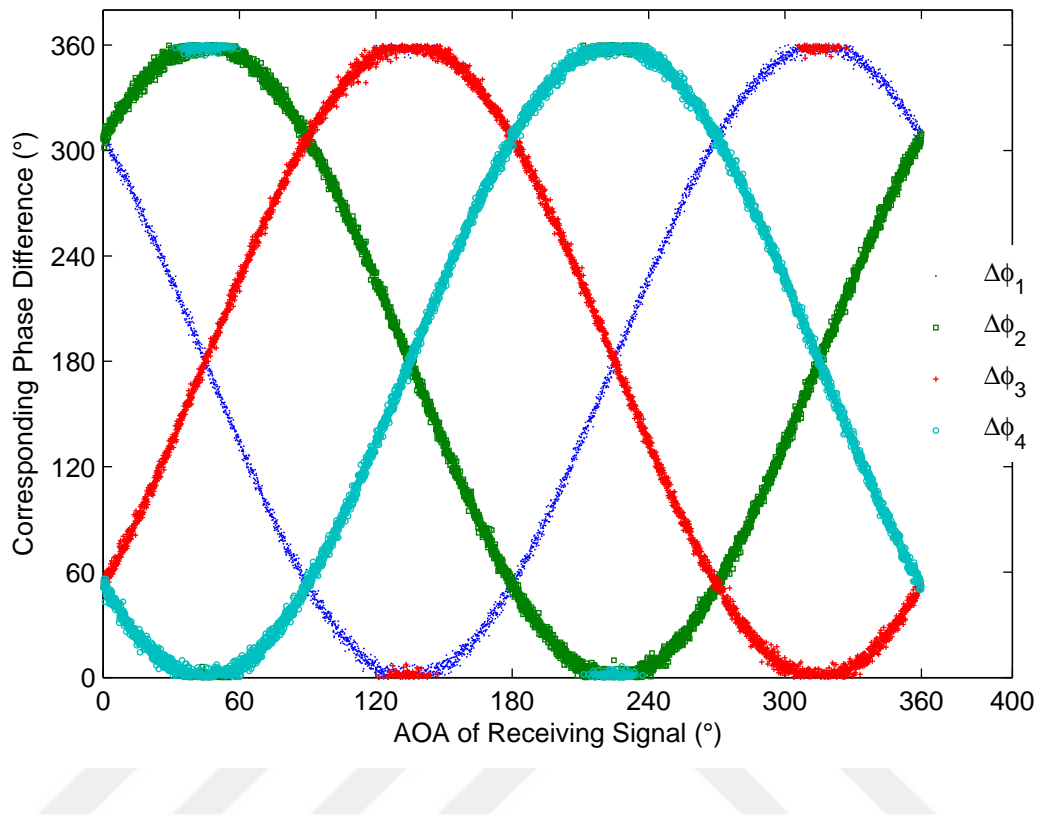
Figure 3.7. Measured Phase Differences Between Antennas 2-1, 3-2, 4-3 and 1-4 with Adding Noise at SNR = 0 dB.

For all possible AOA directions, the system works with actually "0.39°" RMS error. This is because the noise added to signal is wideband and FFT resolves the phase of the given frequency well. In real world, we will face with phase errors due to hardware errors, multipath effects and mutual coupling of antennas. Thus, we can add noise to measured phase differences to simulate an actual FFT based direction finding system.

3.3.3. Hardware Implementation with SDR

In this section, we describe how we can implement the hardware of the proposed system in a Software Defined Radio (SDR) environment. Figure 3.8 is the Block Diagram of Software Defined Radio Platform that can be used to implement interferometer based Radio Direction Finding Systems. It can be also used as the hardware of FFT

MULTI CHANNEL INTERFEROMETER RDF SYSTEM
HARDWARE BLOCK DIAGRAM

Antenna Array
(*n* elements)

AOA

DF Processor

nx2 RF Switch

2 Phase Coherent
Receivers

2 channel ADC
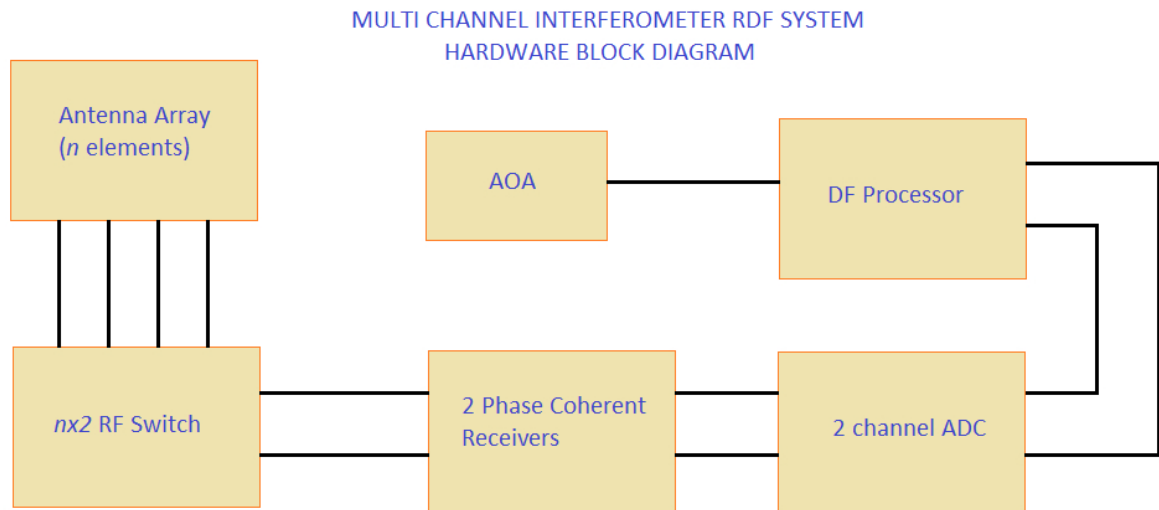
Figure 3.8. Block Diagram of Software Defined Radio Platform that can be used to implement FFT Based Direction Finding System.

Based Correlative Interferometer Method which will be discussed in the rest of the chapter. The most important factor for the system is the matched RF downconverters. In other words, RF downconverters should have to use the same Local Oscillator (LO). In addition, ADCs should use the same clock and can give the samples of the same portions of the data of both channels. Then, digital data is taken by DF processor that can be a Digital Signal Processor or a PC. DF Processor calculates the phase differences between the antennas with the method defined to it.

Hardware implementation of an interferometer based RDF system can be carried out by using Commercial off-the Shelf (COTS) products, e.g., National Instruments' PXI (PCI eXtensions for Instrumentations) based modules. Since, PXIe-5601 modules take LOs from a frequency synthesizer, one can match 2 PXIe-5601 RF downconverter modules by using a common Frequency Synthesizer. 2 PXIe-5622 IF Digitizers can be used to realize 2 channel ADCs. One can also implement this system by using other COTS cards. The important point for the system is to use a common clock and a common oscillator.

3.4. Effect of Antenna Aperture on DF Accuracy

In this section, we will investigate the effect of the antenna aperture on the performance of the FFT Based Correlative Interferometer Method. For wideband operation of an antenna array, different antenna apertures with respect to SOI's wavelength are present. Thus, the effect of the antenna aperture on the DF System's performance is crucial.

Figure 3.9. Measured vs Expected AOA with Noise (Variance of Noise $= 5°$) for $d = \lambda/2$.

Figure 3.9 shows the Measured vs Expected AOA with noise added to phase differences (variance of noise $= 5°$) for $d = \lambda/2$. For Monte Carlo simulations with 100 runs, the rms error of the system is obtained to be "1.84°".

All simulations done so far are for $d = \lambda/2$. Now, let us proceed with $d = \lambda/4$:
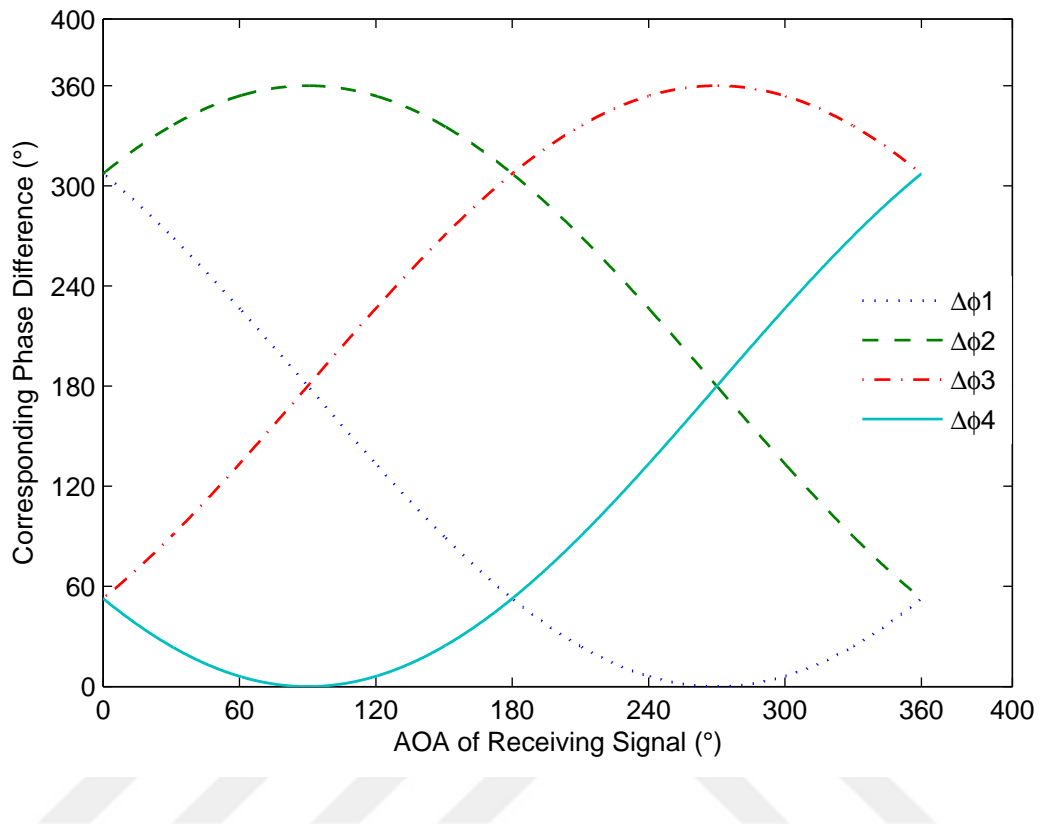
Figure 3.10. Calculated Phase Differences Between Antennas 2-1, 3-2, 4-3 and 1-4 for $d = \lambda/4$.

As we decrease the antenna aperture from $\lambda/2$ to $\lambda/4$, the phase differences between antennas also decreases to half of the former value as seen in Figure 3.10.

Let us try the same cases that are done for d = $\lambda/2$. Firstly, add noise to received signals from antennas with "0" dB SNR. The rms error for this case is "0.8092°". It is approximately twice that of $\lambda/2$. The second case is to add white Gaussian noise with a variance of 5 to phase differences. After doing the same simulation for 100 times, the rms error of the system under this condition is "4.37°". It is approximately "2.4" times of the rms error of $\lambda/2$.

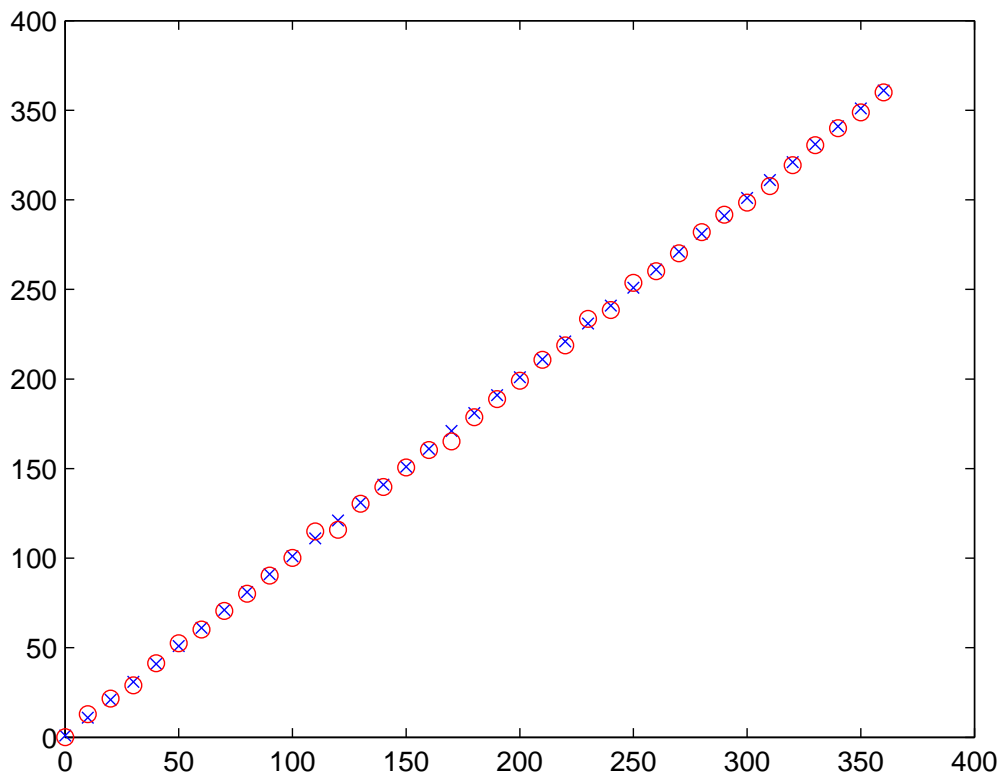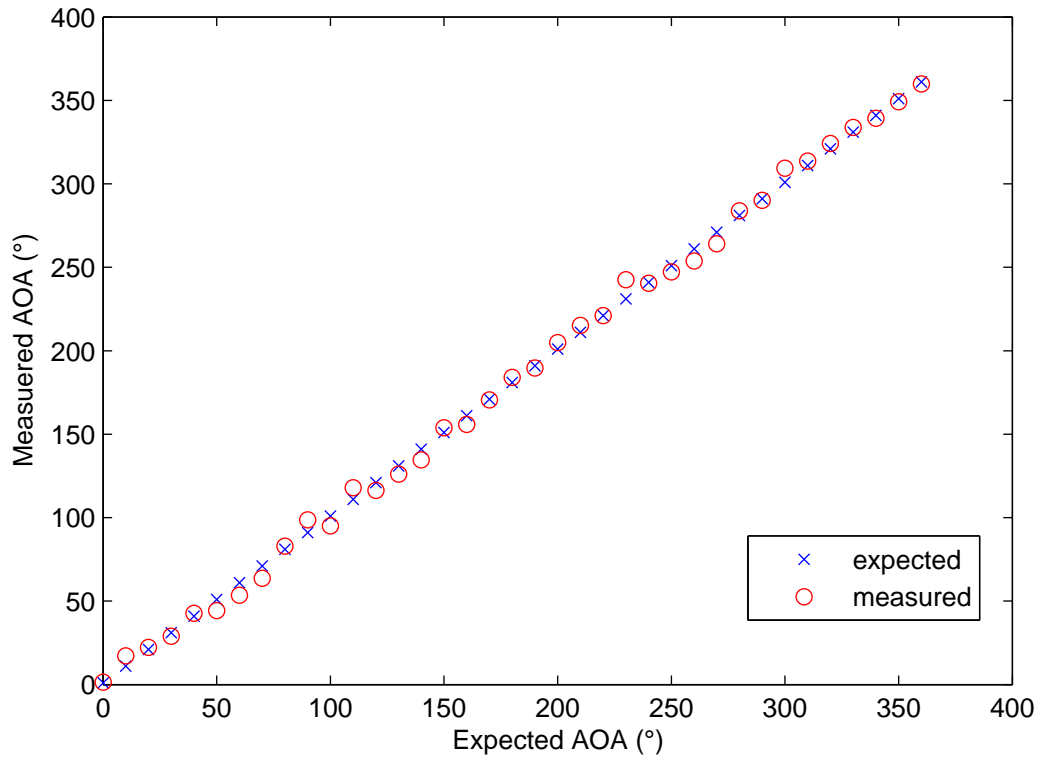Figure 3.11. Measured vs Expected AOA with Noise (Variance of Noise = 5°) for
$d = \lambda/4$

Figure 3.11 shows the Measured vs Expected AOA with noise added to phase differences (variance of noise = 5°) for the antenna aperture $d = \lambda/4$. Performance decrease of the system can be observed by comparing Figure 3.11 and Figure 3.9.
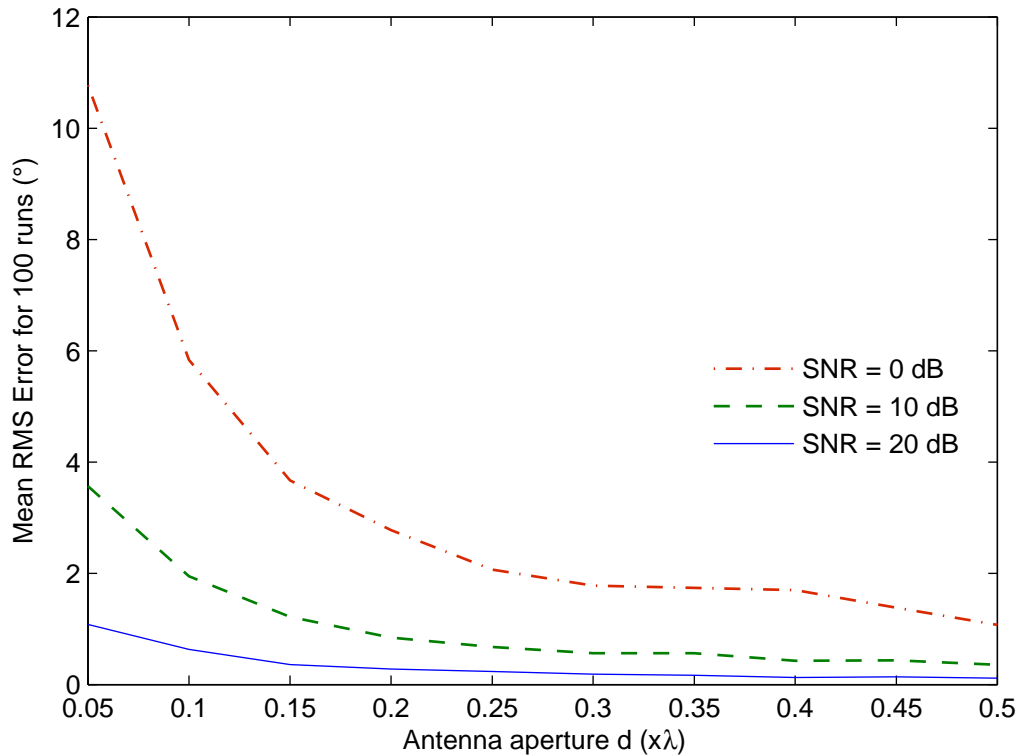
Figure 3.12. RMS Error vs Antenna Aperture with Different Signal-to-Noise Ratios

Figure 3.12 is the graph of the RMS Error vs antenna aperture with different signal-to-noise ratios (0-10-20 dB). As it can be easily seen that increases in the antenna aperture and SNR (signal-to-noise ratio) provides increased system performance.

3.5. Increasing the Antenna Aperture Over Half Wavelength of SOI

Now, go on for $d = \lambda$ and see what happens when the antenna aperture becomes higher than the half wavelength of the signal of intercept.
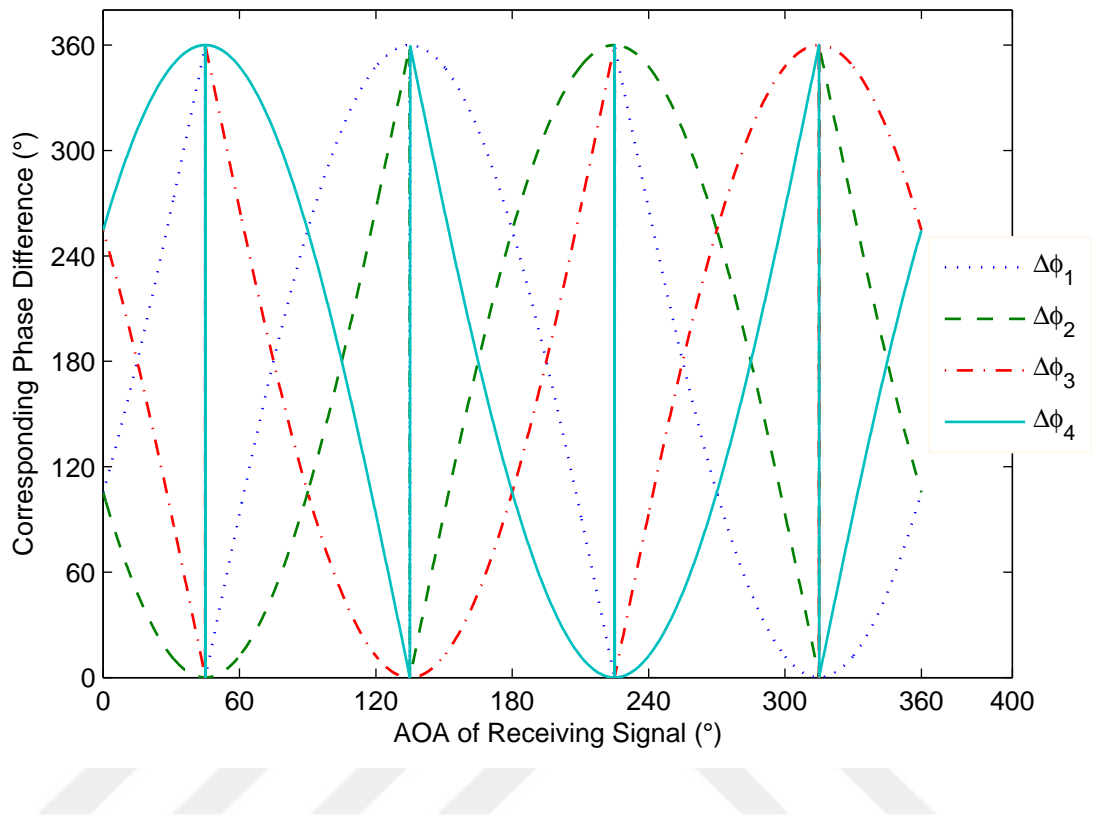
Figure 3.13. Expected Phases of the Signals at the Antennas vs AOA of Incoming Signal for $d = \lambda$

Figure 3.13 shows the expected phases of the signals at the antennas vs AOA of incoming signal for the antenna aperture $d = \lambda$. Phase differences between antenna elements have become more complicated and all phase differences can be same for different angle of arrivals. Thus, the system cannot resolve in which angle the wave is coming from.

Calculated phases of the signals at the antennas vs AOA of incoming signal for the antenna aperture $d = \lambda$ is shown in Figure 3.14.

Figure 3.13, 3.14 and 3.15 show that we cannot resolve the ambiguity by adding offset only. Thus, we require an alternative technique to remedy the situation.
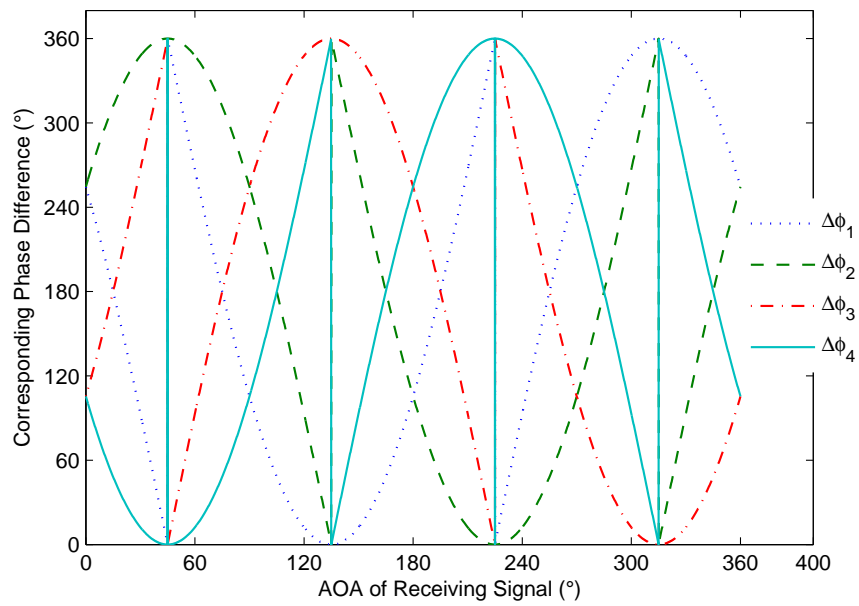
Figure 3.14. Calculated Phases of the Signals at the Antennas vs AOA of Incoming Signal for $d = \lambda$
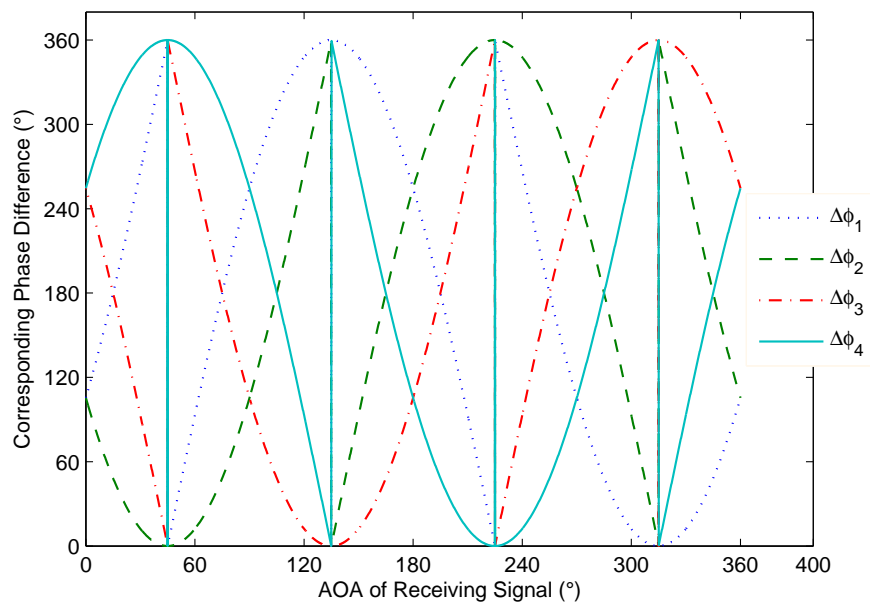
Figure 3.15. Calculated Phases of the Signals at the Antennas vs AOA of Incoming Signal for $d = \lambda$ (Offset Added)
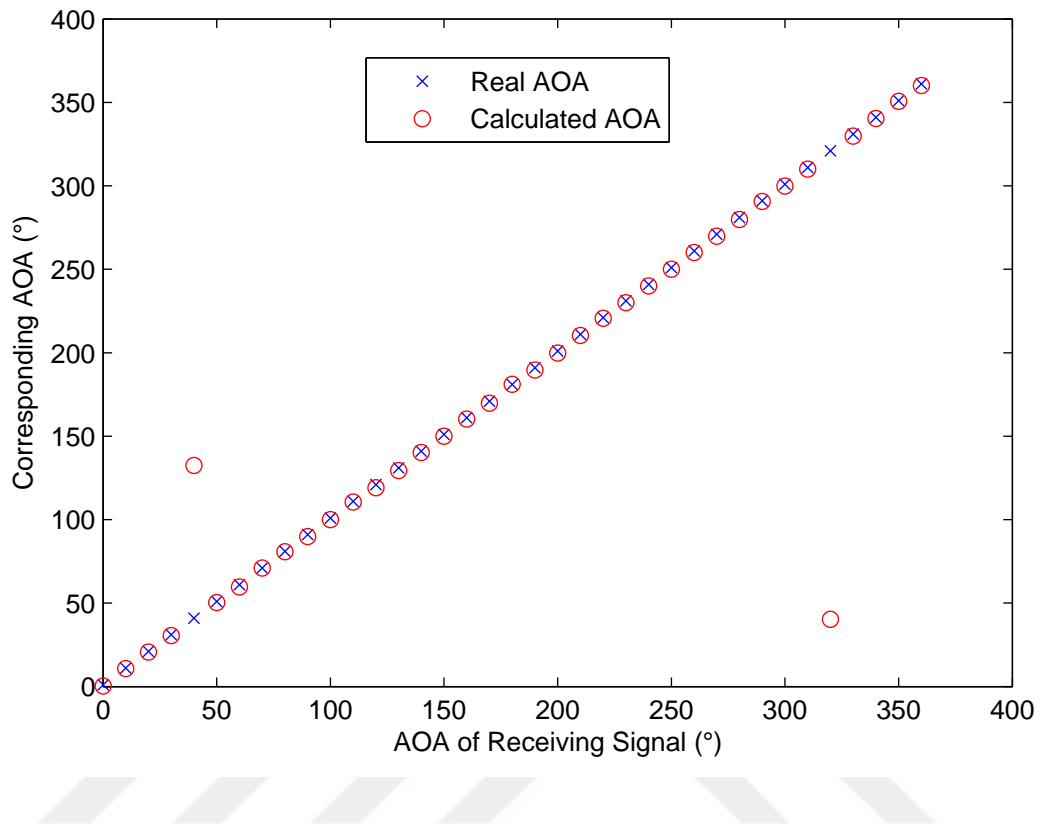
Figure 3.16. Expected vs Calculated AOA for $d = 0.75\lambda$ with an SNR of 5 dB (4 antenna case)

Figure 3.16 shows expected AOA versus calculated AOA for an antenna aperture of $d = 0.75\lambda$ with an SNR of 5 dB. It can be easily seen that AOA at 40° and 320° cannot be resolved due to the ambiguity resulting from antenna aperture greater than $\lambda/2$.
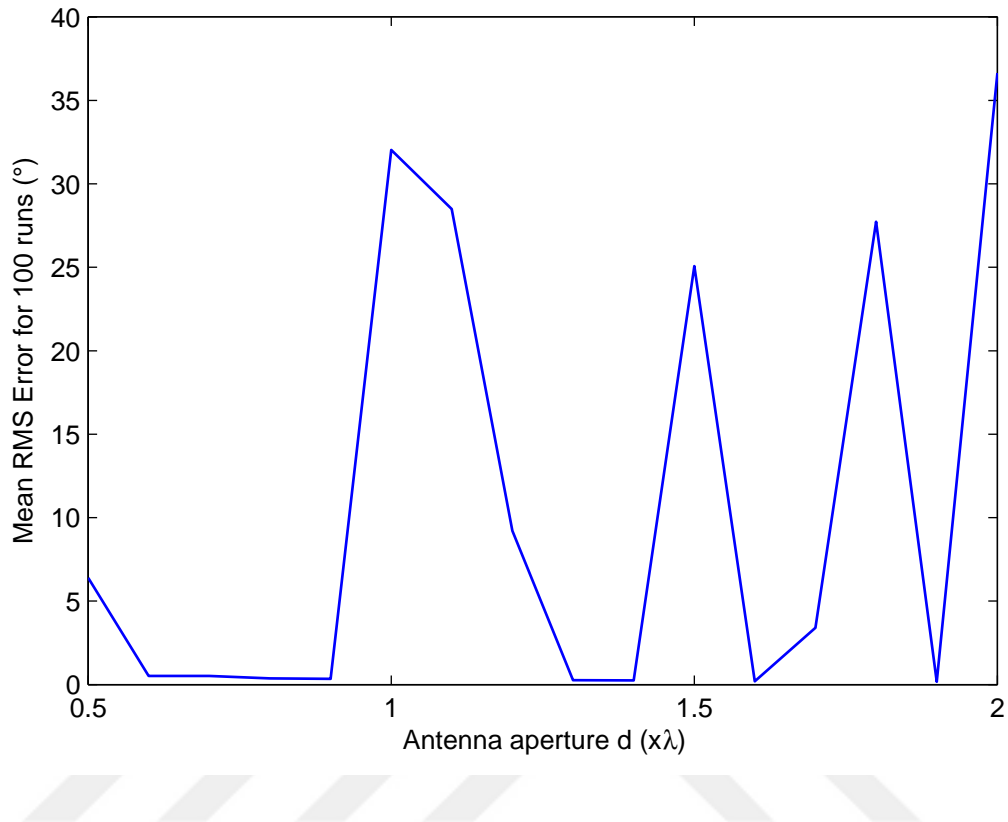
Figure 3.17. RMS Error vs Antenna Aperture from 0.5 λ to 2 λ with an SNR of 5 dB

The ambiguity caused from the greater antenna aperture from $\lambda/2$ is shown in Figure 3.17. Correlative interferometer can solve the ambiguity at some antenna apertures but it is also unsuccessful at some apertures. In some frequencies that correspond to greater antenna aperture than $\lambda/2$, unambiguous AOA estimations are obtained because there is no identical phase difference vectors corresponding to 2 or more AOA for those frequencies and antenna apertures. The correlation of the expected and measured phase differences results in one angle which is the correct AOA, thus ambiguity does not occur.

3.6. Ambiguity for Larger Antenna Apertures

In this section, we will try to solve the ambiguity problem occurring for larger antenna apertures than the half wavelength of the SOI.
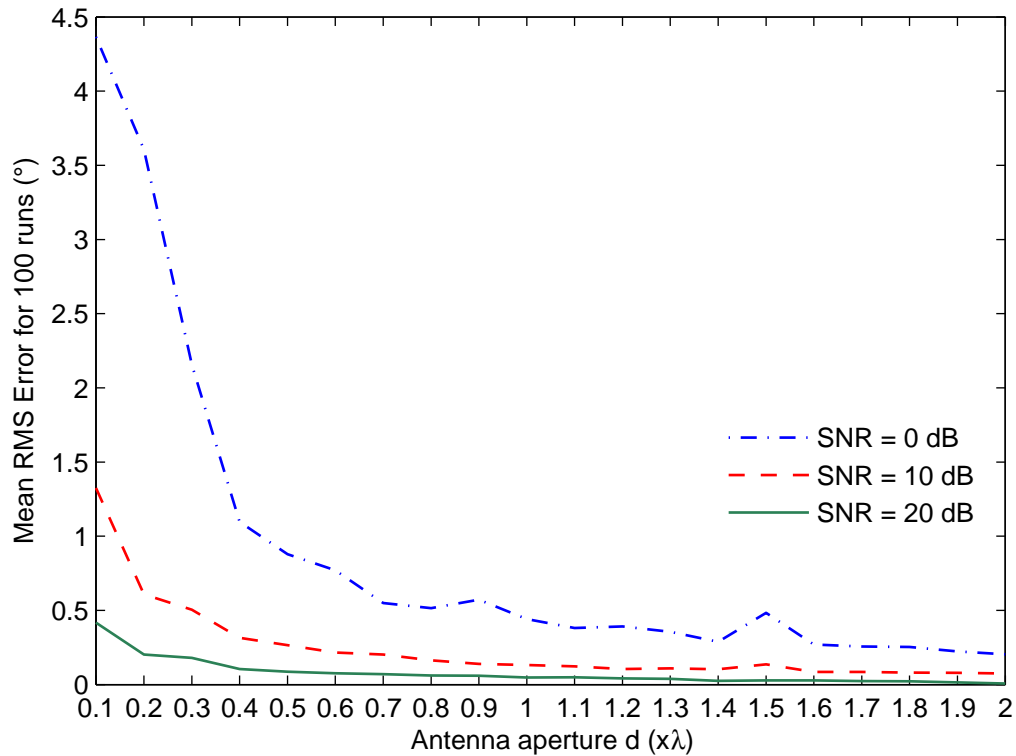
Figure 3.18. RMS Error vs Antenna Aperture with Different Signal-to-Noise Ratios for 5 Antenna System.

In a 4 antenna case, we have actually 2 baselines. Antenna pair 1-2 is parallel to antenna pair 3-4 and antenna pair 2-3 is parallel to antenna pair 4-1. Due to this parallelism we have actually two baselines. Trying to increase baselines can resolve the ambiguity because the probability of the same phase difference for more than 1 angle of arrival will be decreasing with the increase of the baselines which are not parallel to each other.

In order to increase the number of un-parallel baselines, we can increase the number of symmetric antennas in the system. Let us try the case for a 5 antenna system. The system with 5 antennas has 5 un-parallel baselines. Adding 1 antenna to 4 antennas increases the number of un-parallel baselines from 2 to 5. Thus, this should give a better solution for the antenna aperture greater than $\lambda/2$.
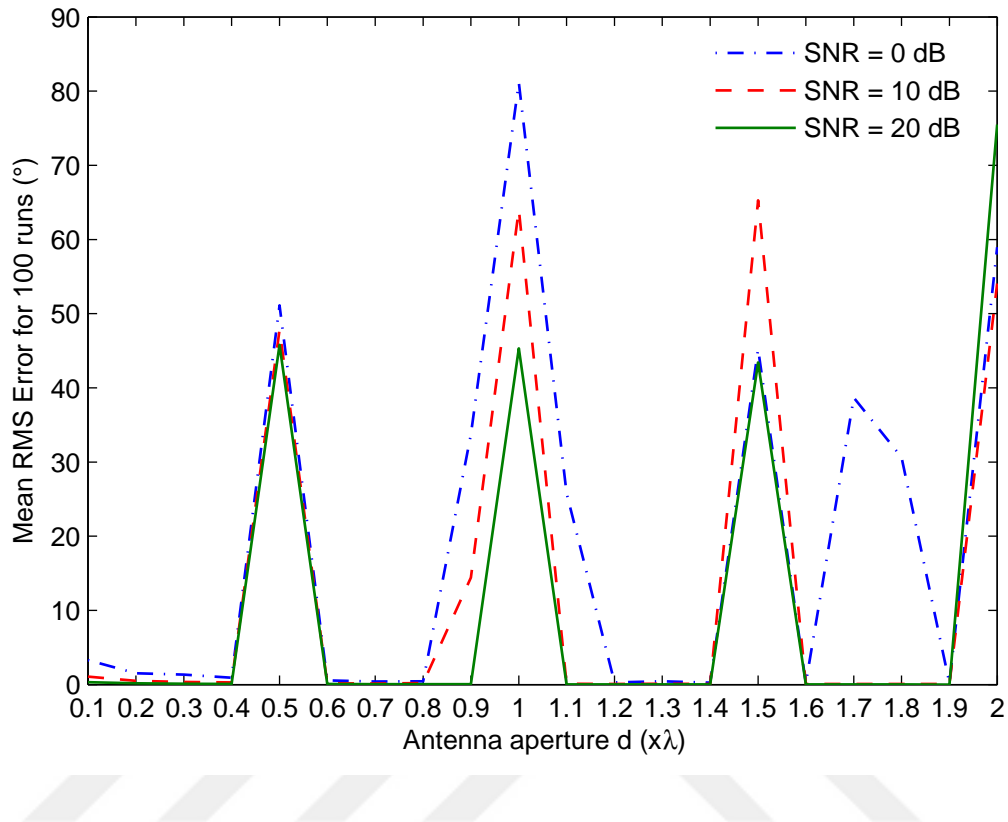
Figure 3.19. RMS Error vs Antenna Aperture with Different Signal-to-Noise Ratios
for 6 Antenna System.

Figure 3.18 shows the RMS error versus antenna aperture for SNR values of
0-10-20 dB for symmetric 5 antenna (pentagon) system. This shows that using 5 non-parallel baselines can solve the ambiguity resulting from the antenna aperture greater
than $\lambda/2$.

In order to see the effect of further increasing the number of antennas, consider
a 6 symmetric antenna system. It should be noted that 6 antenna system has 3 non-parallel baselines. In the 5 antenna case it has 5 non-parallel systems.

Figure 3.19 shows the RMS error versus antenna aperture for SNR values of
0-10-20 dB for symmetric 6 antenna (hexagon) system. This shows that using 3 non-parallel baselines cannot solve the ambiguity resulted from the antenna aperture greater
than $\lambda/2$. In contrast the to 5 antenna system, 6 antenna system cannot resolve the
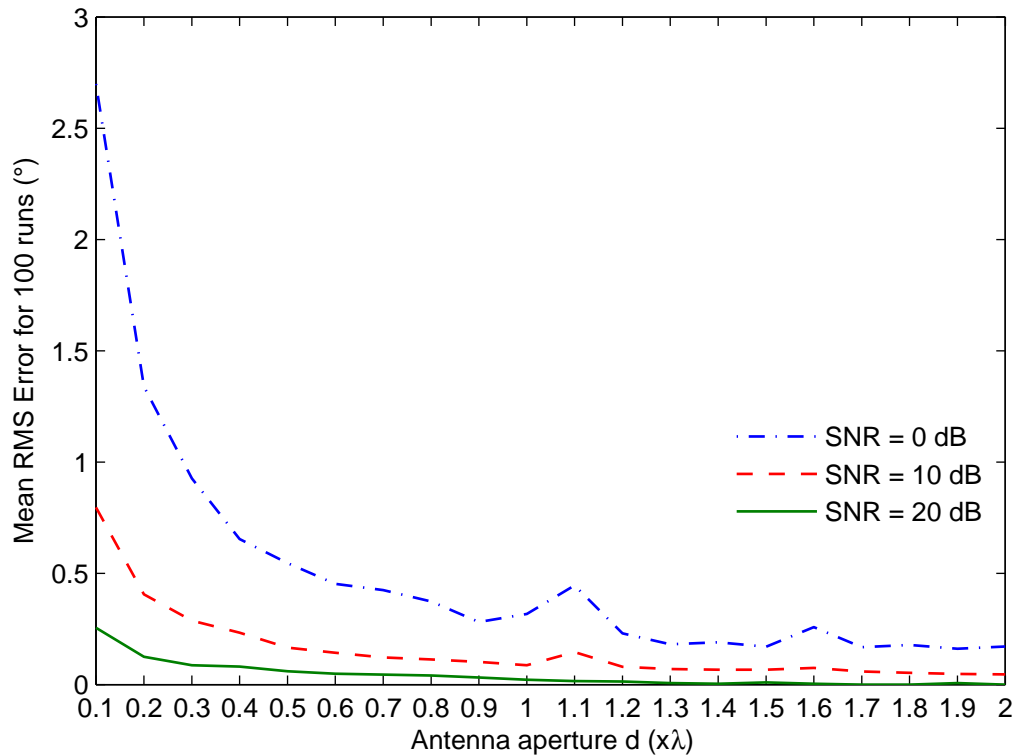
Figure 3.20. RMS Error vs Antenna Aperture with Different Signal-to-Noise Ratios for 7 Antenna System.

ambiguity.

Figure 3.20 shows the RMS error versus antenna aperture for SNR values of 0-10-20 dB for symmetric 7 antenna system. This shows that using 7 non-parallel baselines can solve the ambiguity resulting from the antenna aperture greater than $\lambda/2$ analogous to the 5 antenna system. In contrast to 4 and 6 antenna systems, 5 and 7 antenna systems can resolve the ambiguity.

Figure 3.21 shows the RMS error versus antenna aperture for SNR values of 0-10-20 dB for symmetric 8 antenna system. The 8 antenna system has 4 non-parallel baselines. This shows that using 4 non-parallel baselines can solve the ambiguity resulted from the antenna aperture greater than $\lambda/2$ as the 5 and 7 antenna systems. In contrast to 4 and 6 antenna systems, 5, 7 and 8 antenna systems can resolve the
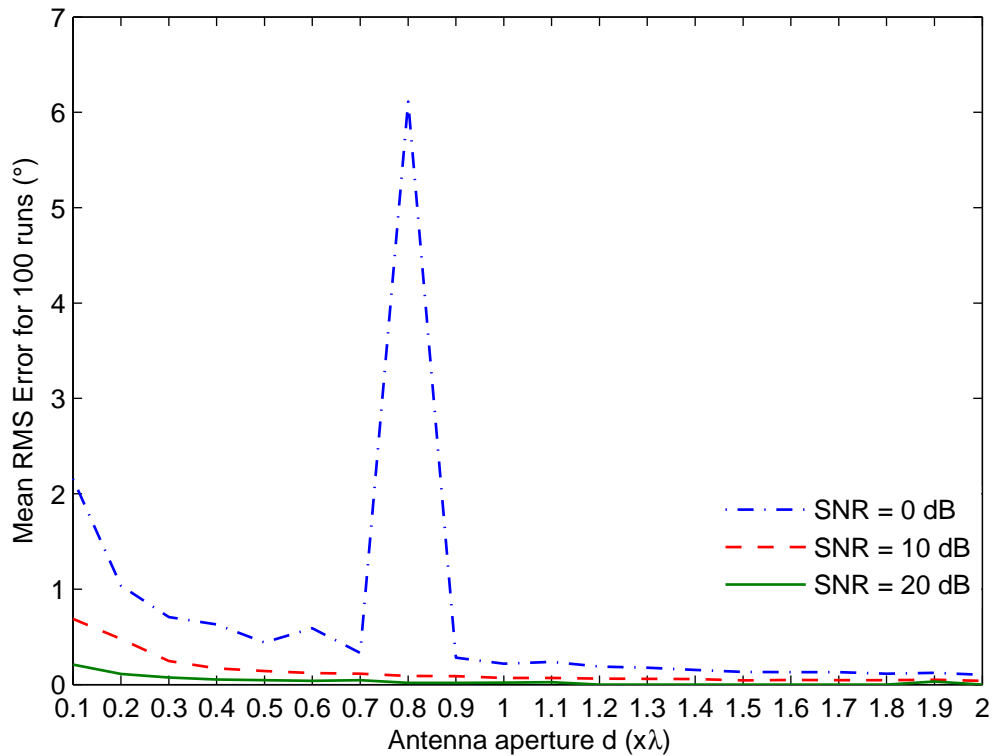
Figure 3.21. RMS Error vs Antenna Aperture with Different Signal-to-Noise Ratios
for 8 Antenna System.

ambiguity.

For 0 dB SNR at an antenna aperture of 0.8 wavelength at one or 2 runs ambiguity
has occurred but it is not very important compared to 4 and 6 antenna systems. Thus,
we can say that 5 and 7 antenna systems have more success in solving ambiguity due
to antenna aperture greater than half of the wavelength.

Figure 3.22 shows the comparison of the 4, 5, 6, 7, 8 antenna systems versus
antenna aperture. Antenna aperture changes from 0.1 λ to 0.5 λ because 4 and 6
antenna systems cannot resolve the ambiguity. It is observed that as the number of
the antennas in DF system increases, the RMS error of the system decreases, in other
words, the system performance increases with the increase of the antenna elements in
a direction finding system.
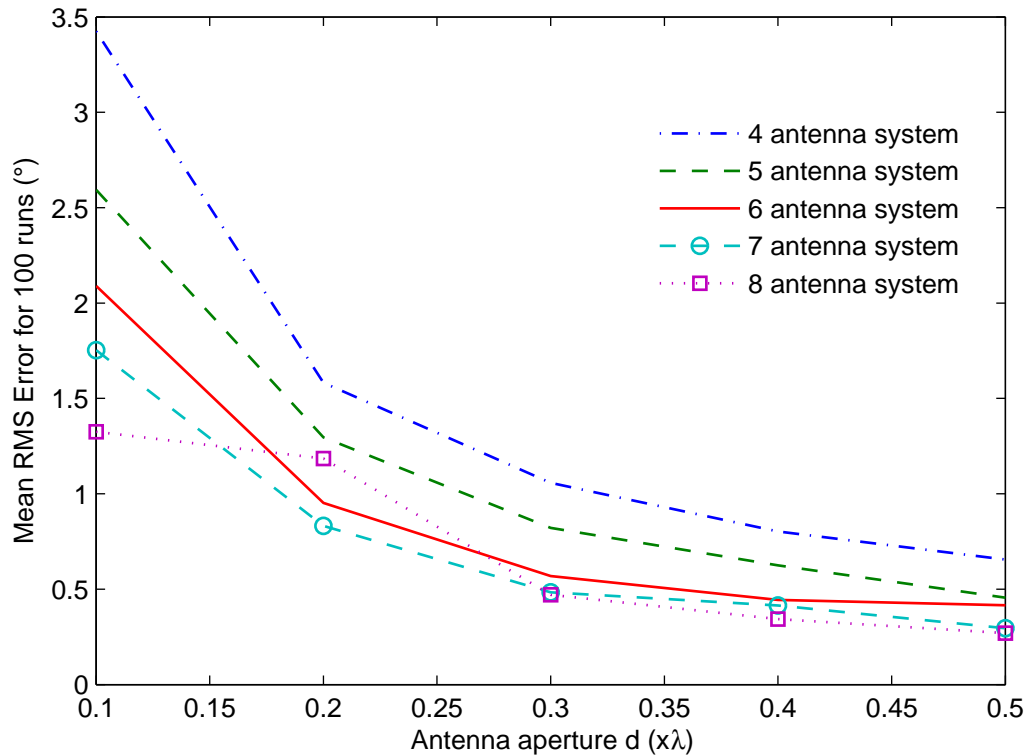
Figure 3.22. RMS Error vs Antenna Aperture for 4, 5, 6, 7, 8 Antenna Systems at an SNR of 5 dB.

3.7. Summary of the Chapter & Concluding Remarks

After reviewing the basic direction finding algorithms in Chapter 2, we discuss the multi-channel interferometer methods in detail in this chapter. We review that Fourier transform based interferometer method has many advantages over other methods such as increased sensitivity, reduced effects of amplitude variations, DOA estimation of complete spectrum in a single snapshot. In addition, as discussed in Section 3.1.3, the correlative interferometer method has important advantages over alternative interferometer methods. Combining the power of FFT and Correlative Interferometer Method to implement FFT based Correlative Interferometer Method provides us with the best antenna aperture to reduce the multipath effects and mutual coupling, etc.

In Section 3.3, it is shown that the performance of a DF system using an FFT

based Correlative Interferometer Method increases with the increase of the antenna aperture. On the other hand, if the antenna aperture is greater than the half wavelength of the incoming RF signal, an ambiguity occurs and it causes system to give erroneous AOA outputs.

It is observed that, increasing the number of non-parallel baselines can provide the system with solving the ambiguity at an antenna aperture greater than the half wavelength of the incoming RF signal. 5 non-parallel baselines actually solve the problem for an antenna aperture of 2 times of the incoming signal wavelength.

Table 3.1. Number of the Symmetric Antennas in a DF System vs the Size of Antenna Array.

Number of antennas	Radius of the Antenna Array (*wavelength (λ))
4	0.353553391
5	0.425325404
6	0.5
7	0.576191218
8	0.653281482

The second important conclusion from the experiments and simulations is that increasing the number of the antennas in a DF system, increases the system performance as well. On the other hand, increasing the number of the antennas in the antenna array of the DF system also increases the size of the antenna array for the same frequency band.

Table 3.1 shows the size of the antenna array with respect to the antenna elements in the system. An 8 antenna element system is 2.36 times greater than 5 antenna element system, where all antenna apertures are equal to the half of the wavelength of the incoming signal, in spite of the fact that the 5 antenna element system is more powerful to solve ambiguities.

Using prime number of antennas in a DF system has been proposed for resolving the ambiguity [32]. In this work, we propose to increase the number of non-parallel baselines to overcome the same problem. In addition, we can conclude that using prime number of antennas maximizes the number of non-parallel baselines in the system. In most cases, maximizing the number of non-parallel baseline is advantageous than using prime number of antennas. For example, the lowest prime number greater than 7 is 11, so 11 antenna system is to be chosen if more than 7 antennas are preferred due to the prime number restriction. However, an 8/9 antenna system can solve the ambiguity with lower antenna array diameter.
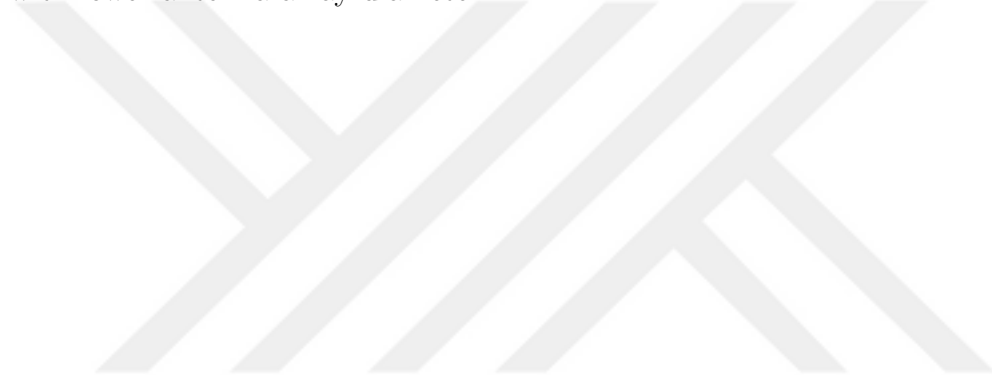
4. SMART ANTENNAS

4.1. Introduction to Array Antennas & Beamforming

An antenna is an electrical device that converts electrical power to electromagnetic waves and vice versa [33]. Antennas are divided basically into two categories: omnidirectional and directional antennas. An omnidirectional antenna, named also as isotropic antenna, has equal gain in all directions. To clarify this statement, an omnidirectional antenna radiates equal amount of power in all x-y-z directions. On the other hand, a directional antenna has a maximum gain (maximum power transmission) in a certain direction and lower gains in other directions. The gain of a directional antenna is described with respect to the gain of an isotropic antenna at the measured frequency [33–35]. For example, a directional antenna with a 5 dBi gain radiates 5 dB more power in its direction respect to the isotropic antenna at that frequency.
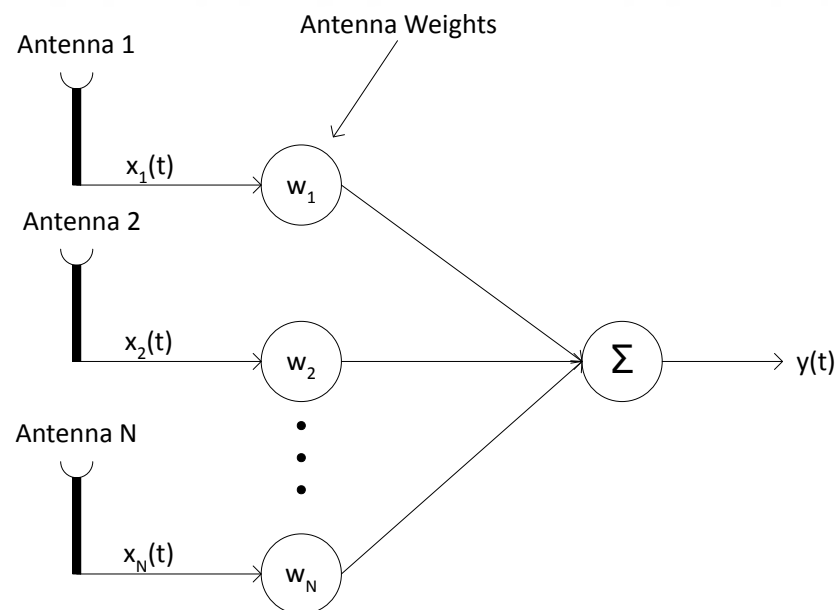
Figure 4.1. Basic Antenna Array System.

An array of antennas can be used to form a phased array antenna. Different phase delays are added to the signals induced on each antenna element of the array and then
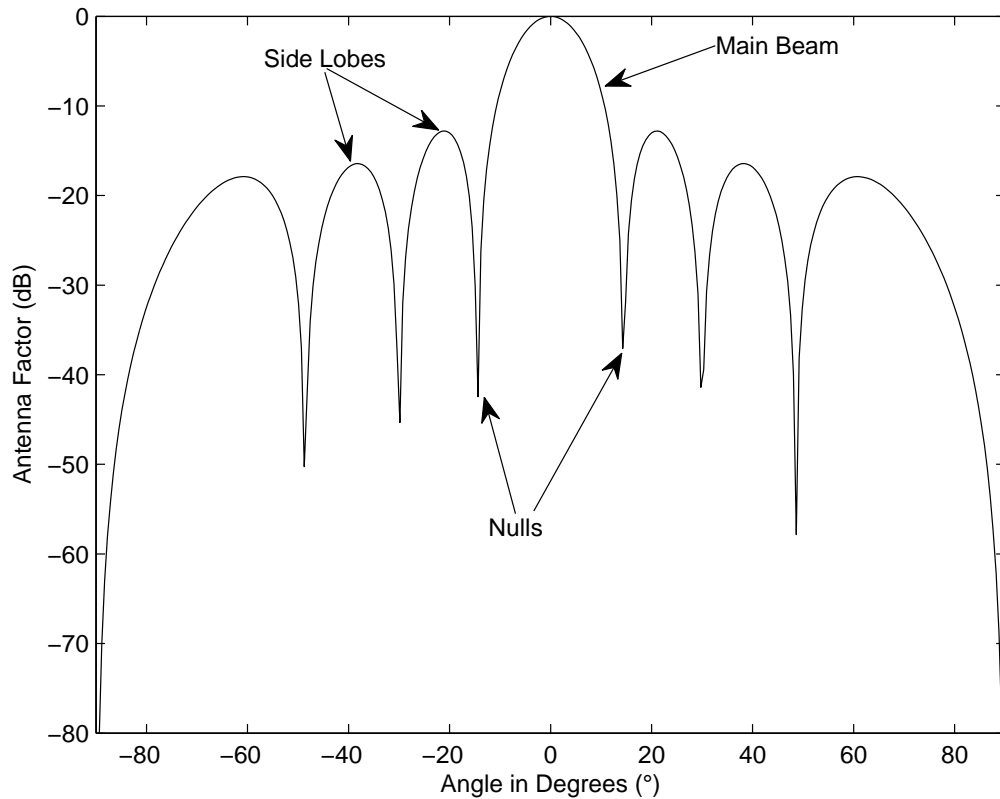
Figure 4.2. Power Pattern of An Eight Element Linear Antenna Array.

combined to create an array output that has a maximum gain in the desired direction. This process is referred to as beamforming. Figure 4.1 shows the block diagram of a general beamforming network. The direction of the maximum gain of the antenna array is defined as beam-pointing direction. For a linear antenna array, if no phase delays are applied to all antenna elements, the beam-pointing direction of the array is perpendicular to the line that all antenna elements are placed along. One can change the beam-pointing direction of the array to the desired direction by adding different phase delays to each element of the array. The system that can dynamically adjust the beam-pointing direction of the array by applying phase delays to the antenna elements is called a *Smart Antenna* [35, 37]. There is a tremendous need and increase in use of smart antennas with the growth of mobile networks.

Figure 4.2 shows the power pattern of an N element Linear Antenna Array in

which all antenna elements are combined to create the array without any phase compensation. Thus, the beam-pointing direction of the array is 0°. The beam in the direction of the beam-pointing is called the *Main Beam*. The beams with lower gains in both sides of the main beam are called *Side Lobes*. Note also that there are local minima, i.e., the array has locally minimum gains at these so called *Null* points. One can adjust the beam-pointing direction of the array by adding phase delays to the antenna outputs via phase shifters. Therefore, beam-pointing direction of the array can be changed electronically and this process is known as *Beam Steering*. In this way, the gain of the antenna system can be maximized in the direction of incident wave and the SNR of the signal can be maximized. The *null* points can also be adjusted in order to eliminate an interferer signal or noise source with the same process [13, 37, 38].

4.1.1. Signal Model of Beamforming

Consider the antenna array system shown in Figure 4.1 formed with N antenna elements. The array output is created by the summation of the signals from each antenna element that are multiplied by a complex antenna weight. The antenna weights which are designed to form the desired array output, stand for hardware such as filters, phase shifters, amplifiers and attenuators that are not shown in the figure. The expression of the antenna array output is given by

$$y(t) = \sum_{i=1}^{N} w_i^* x_i(t) \tag{4.1}$$

where w_i^* denotes the complex conjugate of the each antenna weight and $x_i(t)$ is the signal at each antenna element. Let

$$w = [w_1, w_2, ..., w_N]^T \tag{4.2}$$

$$x(t) = [x_1(t), x_2(t), ..., x_N(t)]^T \tag{4.3}$$

In vector notation, (4.1) can be represented as

$$y(t) = w^H x(t) \qquad (4.4)$$

where superscript T and H are, respectively, the transpose and the complex conjugate transpose of a vector or matrix; w is the weight vector and $x(t)$ is the signal vector.

The array output power at any time t is defined by the square of the magnitude of the array output as follows:

$$P(t) = |y(t)|^2 \qquad (4.5)$$

By substituting $y(t)$ from (4.4) in (4.5), the power of the array output becomes

$$P(t) = w^H x(t) x^H(t) w \qquad (4.6)$$

$x(t)$ can be modelled as zero mean stationary process; therefore the conditional expectation over $x(t)$ gives the mean output power of the antenna array system for a defined antenna weights vector w, i.e., we have

$$P(w) = E[w^H x(t) x^H(t) w] = w^H R w \qquad (4.7)$$

where $E[\cdot]$ is the expectation operator and R is the correlation matrix of $x(t)$ given by

$$R = E[x(t) x^H(t)] \qquad (4.8)$$

Consider an environment that consists of a signal source $x_s(t)$, an unwanted

interference signal $x_i(t)$ interfering with $x_s(t)$ and a random noise signal $x_n(t)$ including background and electromagnetic noises. Then, the array output $y(t)$ becomes

$$y(t) = y_s(t) + y_i(t) + y_n(t) \tag{4.9}$$

where

$$y_s(t) = w^H x_s(t), y_i(t) = w^H x_i(t), y_n(t) = w^H x_n(t) \tag{4.10}$$

In this case, the array correlation matrices of the signal source, interference signal and noise signal are, respectively, given by

$$R_s(t) = E[x_s(t)x_s^H(t)], R_i(t) = E[x_i(t)x_i^H(t)], R_n(t) = E[x_n(t)x_n^H(t)] \tag{4.11}$$

Furthermore, the correlation matrix for total induced signals on the antenna elements is the sum of the correlation matrices of the target signal, interference signal and noise signal and is given by

$$R = R_s + R_i + R_n \tag{4.12}$$

The output power of the array for the target signal, interference signal, and noise signal are P_s, P_i and P_n, respectively and given by

$$P_s = w^H R_s w, P_i = w^H R_i w, P_n = w^H R_n w \tag{4.13}$$

Interference and noise signals are the unwanted signals at the antenna array and their effects on system performance have to be minimized. The total unwanted noise

signal P_N can be defined as the sum of these signals as

$$P_N = P_i + P_n = w^H R_N w \tag{4.14}$$

where R_N is the correlation matrix of total unwanted noise signal given by

$$R_N = R_i + R_n \tag{4.15}$$

The Signal-to-Noise-Ratio (SNR) of the array output is defined as the ratio of the target signal and the total unwanted noise signal that includes interference signal and noise signal:

$$SNR = \frac{P_s}{P_N} = \frac{w^H R_s w}{w^H R_N w} \tag{4.16}$$

SNR is an important indicator in evaluating the performance of antenna arrays and in comparing the performance of different arrays.

4.2. Fixed Weight Beamforming Approach

The aim of using an antenna array is to maximize the array gain in the desired signal (Signal-Of-Interest (SOI)) direction and to minimize the antenna gain in the direction of unwanted signals that are also usually referred to as Signals-Not-Of-Interest (SNOI). To realize these goals, one should determine the suitable antenna weights, i.e., suitable phase shifts at the antenna elements. Thus, by determining the appropriate antenna array parameters, the antenna pattern is shaped according to the desired criteria. These antenna weights and phase shifts are fixed to some values and used as is; therefore, this approach is known as Fixed Weight Beamforming Approach [35, 40].

In order to achieve the beam pattern shape that has a maximum in the direction of SOI and has minima in the directions of SNOIs, there are four basic methods:

- Maximum Signal-to-Interference-Ratio [38, 41]

- Minimum Mean-Square Error [40]

- Maximum Likelihood [42, 43]

- Minimum Variance [24]

4.2.1. Maximum Signal-to-Interference-Ratio Method

Maximum Signal-to-Interference-Ratio Method depends on maximizing the Signal-to-Interference-Ratio (SIR) of the array output. This can be done by maximizing the gain of the array in the direction of SOI and minimizing the gain of the array in the directions of the SNOIs [38, 41]. To realize this goal, the array output in the SOI direction should be 1, and 0 in the directions of SNOIs.

Suppose that the matrix steering vector of the array is given by

$$A = [a_0 \ a_1 \ ... \ a_k] \qquad (4.17)$$

where k is the total number of SOI and SNOIs. Without loss of generality, let the index 0 refer to SOI, and indices $1, 2, ...k$ represent the SNOIs. By using (4.10) and (4.17), we have

$$
\begin{aligned}
y_s &= w^H a_0 &= 1, \\
y_j &= w^H a_j &= 0, \quad j = 1, 2, ...k
\end{aligned}
\qquad (4.18)
$$

By defining $u = [1 \ 0 \ ... \ 0]^T$, the above set of equations can be represented as

$$w^H A = u^T \qquad (4.19)$$

which can be solved for w^H as

$$w^H = u^T A^{-1} \qquad (4.20)$$
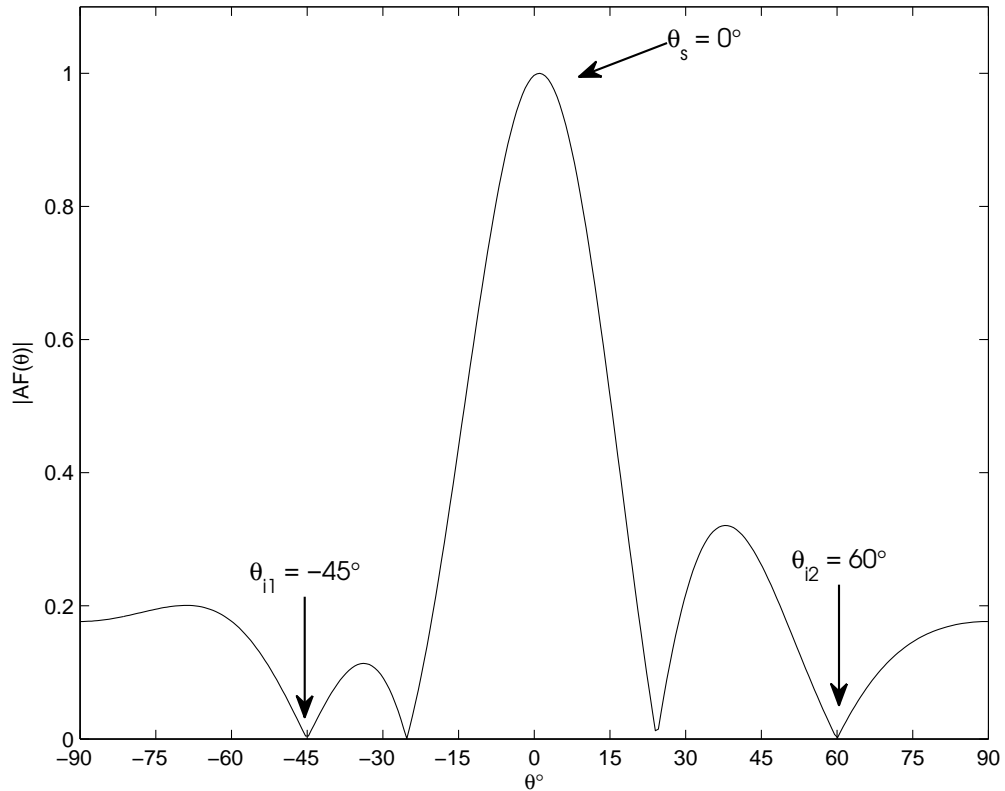
Figure 4.3. Power Pattern of Antenna Array with SIR side-lobe cancelling.

The above equation relies on the assumption that the matrix A is square and invertible. In the case of the number of inputs (signal and interferer) is less than the number of antennas, Godara has suggested the following formula to estimate the antenna weights [21]

$$w^H = u^T A^H \left(A A^H + \sigma_n{}^2 I \right)^{-1} \tag{4.21}$$

where the noise variance $\sigma_n{}^2$ is added to equation in order to avoid singularity in matrix inversion.

Figure 4.3 shows the power pattern of the three element linear antenna array using *Maximum SIR* method with SOI in the $\theta_s = 0°$ and SNOIs in the directions of

$\theta_{i1} = 40°$ and $\theta_{i2} = -60°$.

4.2.2. Minimum Mean-Square Error Method

Minimum Mean-Square Error Method depends on optimizing the array weights by minimizing the mean square error (MSE) [40]. The difference of the array configuration from the Maximum SIR method is the reference signal to compare the array output with. The method tries to minimize the error, $\varepsilon(t)$, between the reference signal, $m(t)$, and the array output, $y(t)$:

$$\varepsilon(t) = m(t) - y(t) = m(t) - w^H x(t) \tag{4.22}$$

Then, MSE of the array can be calculated by

$$|\varepsilon(t)|^2 = |\, m(t)|^2 - 2m(t)w^H x(t) + w^H x(t)x^H(t)w \tag{4.23}$$

Taking the expected value of both sides and suppressing the time dependence, we obtain

$$E\left[|\varepsilon|^2\right] = E\left[|\, m^2|\right] - 2w^H r + w^H R_s w \tag{4.24}$$

where the correlations are defined in (4.11), (4.12), (4.15) and r is given by

$$r = E[m \cdot x] = E[m^* \cdot (x_s + x_i + x_n)] \tag{4.25}$$

The minimum value of MSE can be obtained by calculating its gradient with respect to the weight vectors and equating it to zero, i.e.,

$$\nabla_w(E[|\varepsilon|^2]) = 2Rw - 2r = 0 \tag{4.26}$$
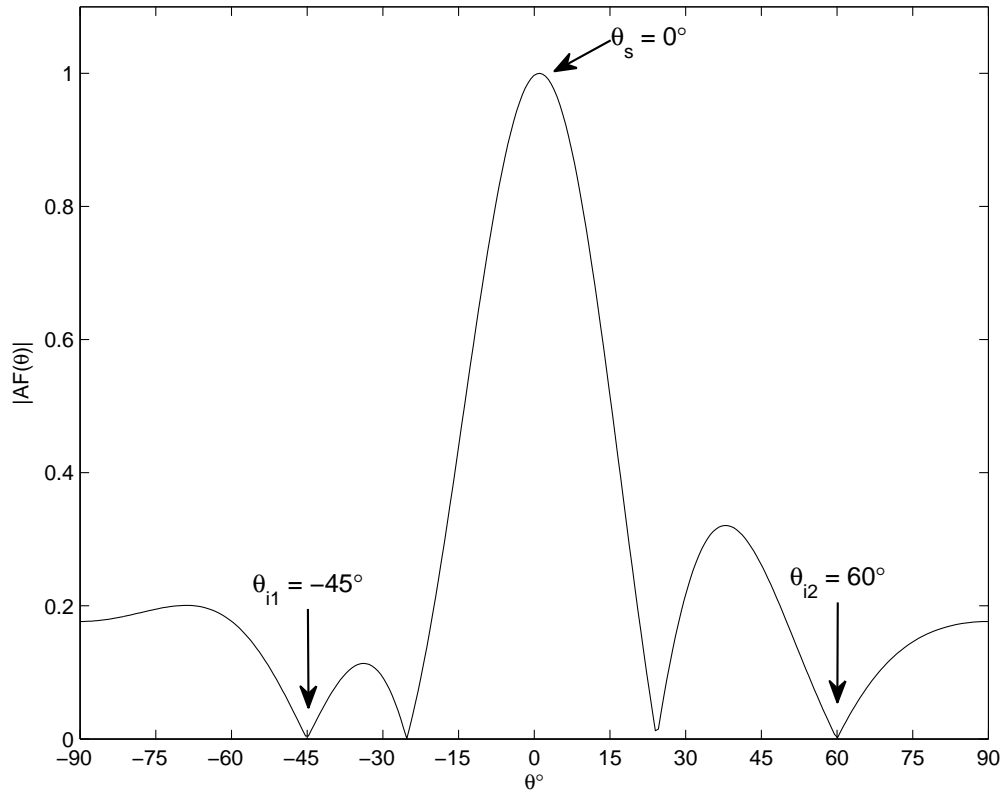
Figure 4.4. Power Pattern of Antenna Array with MSE side-lobe cancelling.

which yields the optimum Wiener solution

$$w_{MSE} = R^{-1} r \tag{4.27}$$

If the reference signal is equal to the desired signal s and interfering signals are uncorrelated with the desired signal, then r can be simplified using (4.17), (4.18) and (4.25) as

$$r = E[s^* \cdot x] = S \cdot a_0 \tag{4.28}$$

where

$$S = E[|s|^2] \tag{4.29}$$

Then, the optimum array weight vector in (4.27) becomes

$$w_{MSE} = SR^{-1} a_0 \tag{4.30}$$

Figure 4.4 shows the power pattern of the five element linear antenna array using *MSE* method with SOI in the $\theta_s = 0°$ and SNOIs in the directions of $\theta_{i1} = 30°$ and $\theta_{i2} = -20°$.

4.2.3. Maximum Likelihood Method

The *Maximum Likelihood Method* relies on assuming an unknown desired signal x_s and unwanted signal x_n that has a zero mean Gaussian distribution. The method aims to define a likelihood function to make an estimation on the desired signal [42,43]. The input signal of the array is given by

$$x = x_s + x_n = a_0 s + x_n \tag{4.31}$$
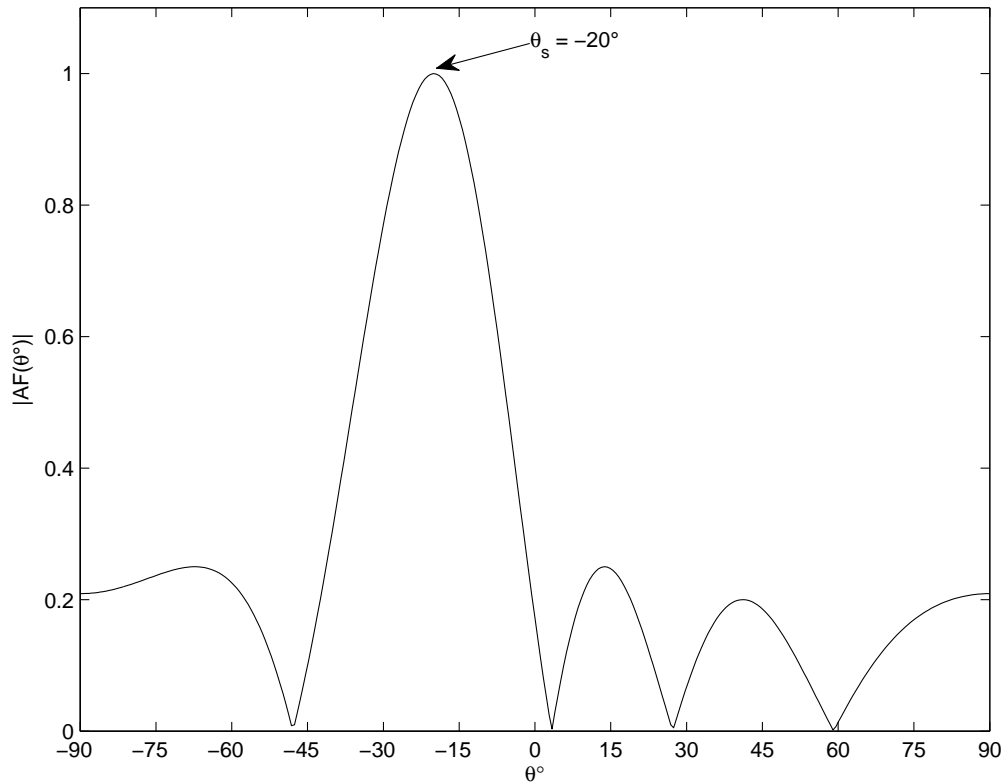
Figure 4.5. Power Pattern of Antenna Array with ML method.

The joint probability density function $p(x|x_s)$

$$p(x|x_s) = \frac{1}{\sqrt{2\pi\sigma_n^2}} e^{-((x-a_0 s)^H R_n^{-1}(x-a_0 s))} \tag{4.32}$$

is the likelihood function and can be used the estimate the desired signal, where σ_n is the standard deviation of noise and $R_n = \sigma_n^2 I$ is the noise correlation matrix.

For simplicity, the log-likelihood function can be defined as the logarithm of the probability density function such as

$$L[x] = -ln\left[p(x|x_s)\right] = C(x - a_0 s)^H R_n^{-1}(x - a_0 s) \tag{4.33}$$

where C stands for the constant terms of the equation. The maximum of the likelihood function $L[x]$ can be found by taking partial derivative with respect to s and equating it to zero, i.e.,

$$\frac{\partial L[x]}{\partial s} = -2a_0^H R_n^{-1} x + 2s a_0^H R_n^{-1} a_0 = 0 \tag{4.34}$$

which yields

$$s = \frac{a_0^H R_n^{-1}}{a_0^H R_n^{-1} a_0} x = w_{ML}^H x \tag{4.35}$$

Thus, the optimum antenna weights for ML method are given by

$$w_{ML} = \frac{a_0^H R_n^{-1}}{a_0^H R_n^{-1} a_0} \tag{4.36}$$

Figure 4.5 shows the power pattern of the five element linear antenna array using *MSE* method with SOI in the $\theta_s = -20°$.

4.2.4. Minimum Variance Method

The last popular method in this category is the *Minimum Variance Method* and it is also usually referred to as the minimum variance distortionless (MVDR) method [44]. Unlike the *Maximum Likelihood Method*, MVDR relies on the assumption of zero mean desired and unwanted signals. The aim of the method is to minimize the noise variance and to provide undistorted desired signal from antenna weights [24]. The array output is given by

$$y = w^H x = w^H a_0 s + w^H u \tag{4.37}$$

For distortionless desired signal output, we should have the array output

$$y = s + w^H u \qquad (4.38)$$

Under the assumption of that SNOI has zero mean, the variance of y is given by

$$\sigma_{MV}^2 = E[|w^H x|^2] = E[|s + w^H u|^2] = w^H R_u w \qquad (4.39)$$

By using the method of Lagrange, the variance can be minimized. A cost function can be defined as a weighted sum of variance and the constraint in (4.37)

$$
\begin{aligned}
J(w) &= \tfrac{1}{2}\sigma_{MV}^2 + \lambda\left(1 - w^H a_0\right) \\
&= \tfrac{1}{2}w^H R_u w + \lambda\left(1 - w^H a_0\right)
\end{aligned}
\qquad (4.40)
$$

where $J(w)$ is the cost function and λ is the Lagrange multiplier.

Since the cost function is quadratic, it can be minimized by setting its gradient to zero, i.e.,

$$\nabla_w J(w) = R_u w_{MV} - \lambda a_0 = 0 \qquad (4.41)$$

$$w_{MV} = \lambda R_u^{-1} a_0 \qquad (4.42)$$

By using the constraint and (4.42) the Lagrange multiplier is computed as

$$\lambda = \frac{1}{a_0^H R_u^{-1} a_0} \qquad (4.43)$$

Minimum variance optimum array weights can be obtained from (4.42) and (4.43) as

$$w_{MV} = \frac{R_u^{-1} a_0}{a_0^H R_u^{-1} a_0} \tag{4.44}$$

4.3. Switched Beamforming

The switched beamforming approach to smart antennas relies on using multiple fixed beams and choosing the most suitable one for the desired signal. A switched beamforming system detects the signal strength at each beam by switching among beams and chooses the one from the predetermined fixed beams that results in the strongest received signal strength. The switched beam systems combine multiple antennas (antenna array) to create multiple directed narrow beams to provide more spatial selectivity that cannot be achieved from a single-element antenna. The configuration of such a system consists of a number of fixed beams one of which is turned on toward the SOI.

The first to be invented and widely-known type of switched beamformed system is Butler Matrix system. It is an $N \times N$ network with N antenna elements connected to the N passive feeding ports and has N outputs. The passive elements are fixed phase shifters and hybrid couplers [39]. N should be a power of 2. The Butler matrix creates N orthogonal beams by performing a spatial fast Fourier transform. The system can cover a sector up to 360° by choosing appropriate antenna elements and appropriate spacing. Each output of the network should be fed to a dedicated receiver or transmitter and the appropriate beam can be selected by using a switch. A Butler matrix can be used in both receive and transmit mode and has 2 different functions:

- distribute RF signals to antenna elements
- provide orthogonal beams.
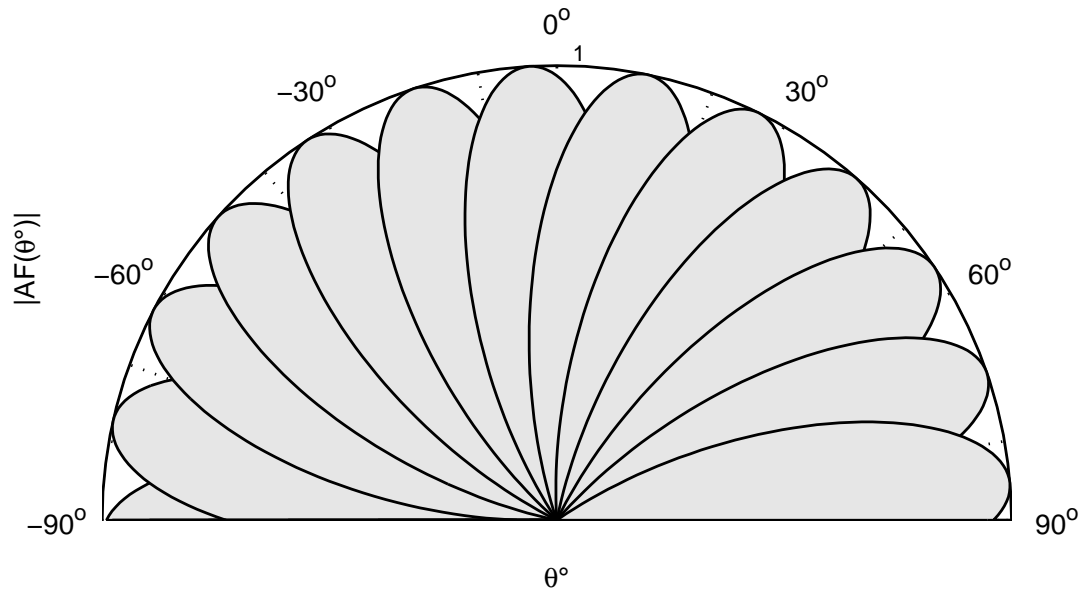
Figure 4.6. Multiple Beam Patterns Created and Used in Switched Beamforming.

Fig. 4.6 shows the multiple fixed beams created and used in a switched beamforming system. The system jumps from beam to beam and measures the received signal strength at each beam. Then, it chooses the optimum one and the system receives the desired signal from this beam.

One of the fixed beam of the multiple fixed beams of a switched beamforming system is shown in Fig. 4.7. This may be the optimum beam to receive the SOI. On the other hand, interferer signals are received by the system with some attenuation. The system has an advantage of greater gain in the direction of SOI with respect to classical antenna systems, however a fixed beamforming scheme that is created for the maximum gain in the SOI direction and side-lobe cancellation in the SNOIs directions yields better results.
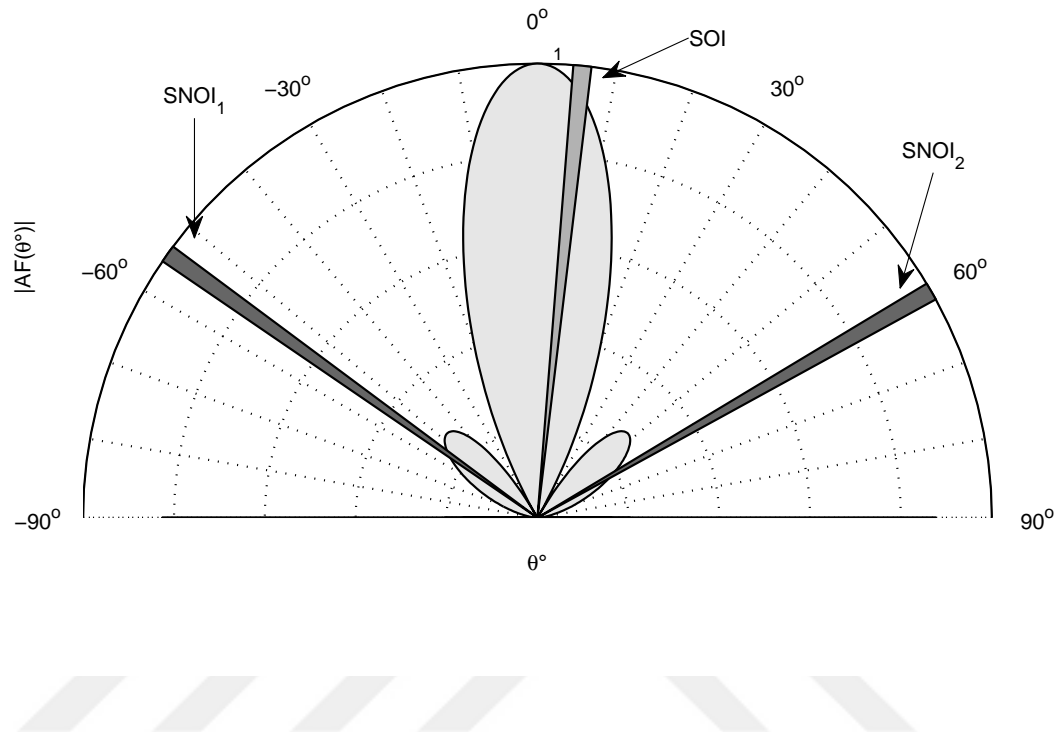
Figure 4.7. One of the Fixed Beam of the Switched Beamforming System

4.4. Adaptive Beamforming

Fixed beamforming methods assume that the desired and undesired signals arrive at fixed angles. If the directions of the signals change with time, a fixed beamforming network cannot adopt itself to new directions. Adaptive beamforming methods are used to solve the problem with the signals that are changing the directions continuously. Adaptive beamforming systems have a feedback network and try to adopt themselves to new conditions in the electromagnetic environment. Adaptation process of these systems uses different optimization schemes. The most popular adaptive beamforming methods are:

- Least Mean Squares
- Sample Matrix Inversion
- Recursive Least Squares

4.4.1. Least Mean-Squares Method

The *Least Mean-Squares (LMS) Method* relies on optimizing the array weights by minimizing the MSE. As discussed in Section 4.2, the method tries to minimize the error $\varepsilon(k)$ between the reference signal $m(k)$ and the array output $y(k)$, and recall that the optimal solution is given by

$$w_{LMS} = R^{-1}r \tag{4.45}$$

The instantaneous array correlation matrix R and the signal correlation vector r are not known a priori and should be estimated by using snapshots at each time instant. The instantaneous estimates of array correlation matrix and signal correlation vector are given by

$$R(k) \approx x(k)x^H(k) \tag{4.46}$$

and

$$r(k) \approx m^*(k)x(k) \tag{4.47}$$

Widrow proposed the following steepest descend method

$$w(k+1) = w(k) - \frac{1}{2}\mu\nabla_w(E\left[|\varepsilon|^2\right] \tag{4.48}$$

to approximate the gradient of the cost function where $E\left[|\varepsilon|^2\right]$ is defined in (4.24). The above equation can be represented as

$$w(k+1) = w(k) - \mu e^*(k)x(k) \tag{4.49}$$

where the error signal is given by $e(k) = m(k) - w^H(k)x(k)$.

The above algorithm converges if the following condition

$$0 \leq \mu \leq \frac{1}{2\lambda_{max}} \tag{4.50}$$

is satisfied where λ_{max} is the largest eigenvalue of the correlation matrix R [38].
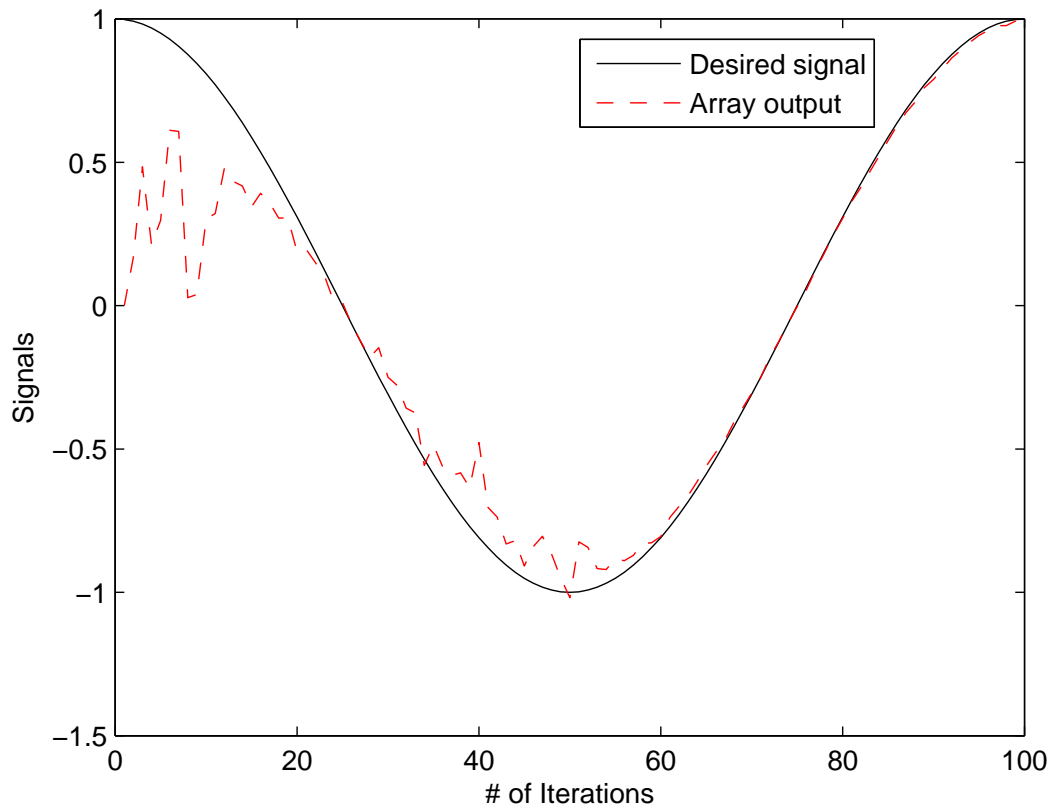
Figure 4.8. The array output of a 5 element linear LMS system

Figs. 4.8 and 4.9 show the output and the antenna weights of an 5 element antenna array used in the LMS adaptive beamforming where the desired signal comes from $30°$ with an interfering signal at $0°$. The system updates its antenna weights at each snapshot. It takes more than 80 iterations for system to stabilize its antenna weights and reach optimum values. In spite of the fact that system can adopt perfectly to the electromagnetic environment, it takes quite a long time for convergence.
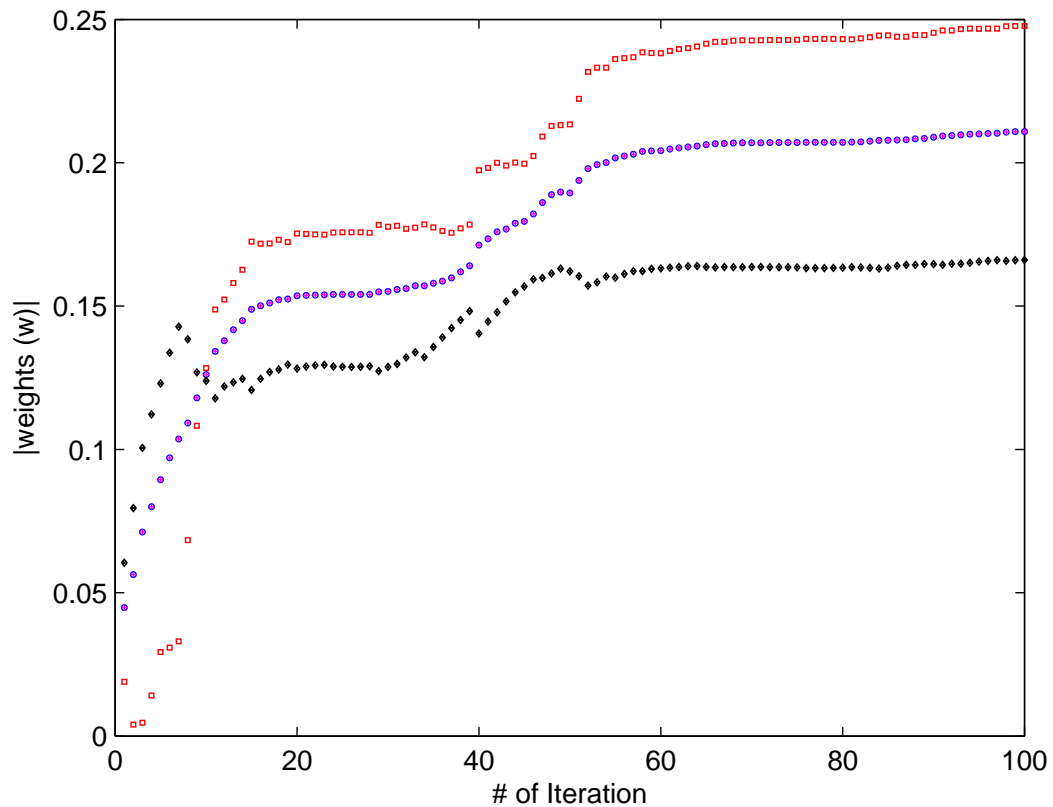
Figure 4.9. Update of Antenna Weights of a 5 element linear LMS system

4.4.2. Sample Matrix Inversion Method

Sample Matrix Inversion (SMI) Method is one way to reduce this relatively long convergence time of the LMS method. SMI method takes time average of the estimate of the array correlation that is known as *sample matrix*. Note that the sample matrix is equal to the real array correlation matrix if the random process is ergodic in the correlation. The time average estimates of the correlation matrix R and the correlation vector r can be evaluated by

$$R = \frac{1}{K} \sum_{k=1}^{K} x(k)x^{H}(k) \tag{4.51}$$

$$r = \frac{1}{K} \sum_{k=1}^{K} d^{*}(k)x(k) \tag{4.52}$$

where K is the number of observation samples.

If we define $X_K(k)$ as the kth block of x vectors ranging over K snapshot as

$$X_K(k) = \sum_{k=1}^{K} x(k) \tag{4.53}$$

then the time average estimates of the correlation matrix and the correlation vector are given by

$$\widehat{R}(k) = \frac{1}{K} X_K(k) X_K^H(k) \tag{4.54}$$

$$\widehat{r}(k) = \frac{1}{K} d^*(k) X_K(k) \tag{4.55}$$

If we substitute (4.54) and (4.55) into (4.27), the SMI weights are obtained as

$$w_{SMI}(k) = R^{-1}(k) r(k) = \left[X_K(k) X_K^H(k) \right]^{-1} d^*(k) X_K(k) \tag{4.56}$$

The SMI method requires less time than the LMS method to a satisfactory degree of convergence of antenna weights [41]. The first disadvantage of the method is how to determine the optimum number for K. The second one is that if there is a rapid change in the direction of desired signal, the convergence time becomes extremely higher than the LMS method [21, 45]. In addition, inverting potentially ill conditioned correlation matrices results in errors and singularities and inverting large matrices requires high computational power.

4.4.3. Recursive Least Squares Method

The computational load and potential singularities reduce the popularity of SMI method. An alternative is to use the *Recursive Least Squares* (RLS) method which calculates the estimates of the correlation matrix and correlation vector recursively. To this end, rewrite the estimates of correlation matrix and correlation vector at the

kth snapshot as

$$\widehat{R}(k) = \sum_{i=1}^{k} x(i)x^{H}(i) \tag{4.57}$$

$$\widehat{r}(k) = \sum_{i=1}^{k} d(i)x(i) \tag{4.58}$$

If we assume that the direction of the signals changes slowly, the values of the last snapshots become more important than the first snapshots. Thus, we may decrease the values of the first samples by using a forgetting factor α [44, 46] as follows:

$$\widehat{R}(k) = \sum_{i=1}^{k} \alpha^{k-i} x(i)x^{H}(i) \tag{4.59}$$

$$\widehat{r}(k) = \sum_{i=1}^{k} \alpha^{k-i} d(i)x(i) \tag{4.60}$$

Here, α should satisfy $0 \leq \alpha \leq 1$. If we choose α equal to 1, the algorithm reduces to ordinary LMS. Decreasing the value of α increases the forgetting speed.

4.5. Summary of the Chapter & Concluding Remarks

Three different beamforming approaches for smart antennas; fixed, switched and adaptive have been discussed in this chapter. Fixed beamforming approach achieves the expected gain in the desired signal direction and side-lobe cancellation in the directions of the unwanted signals. However, it cannot be used in a changing electromagnetic environment. A switched beamforming system switches between the predefined beams and therefore can handle the signals in all directions. It uses fixed beamforming methodology in creating multiple predefined beams. Switched beamforming systems have very fast response to the changes in the direction of the target signals. On the other hand, they can not provide the optimum solution for every combination of desired and unwanted signals due to the limitation of number of the predefined beams. In addition, if the directions of the signals change with time, it cannot adopt itself

to new directions. Adaptive beamforming methods are used to overcome the problem with the signals that are changing the directions continuously. Adaptive beamforming systems have a feedback network and try to adopt themselves to new conditions in the electromagnetic environment.

5. MULTI-MODEL ADAPTIVE BEAMFORMING

Three different beamforming approaches for smart antennas; fixed, switched and adaptive have been discussed in Chapter 4. Recall that the fixed beamforming approach achieves the expected gain in the desired signal direction and side-lobe cancellation in the directions of the unwanted signals. However, it cannot be used in a changing electromagnetic environment. A switched beamforming system switches between the predefined beams and therefore can handle the signals in all directions. It uses fixed beamforming methodology in creating multiple predefined beams. Switched beam-forming systems have very fast response to the changes in the direction of the target signals. On the other hand, as seen in Fig. 4.7, they can not provide the optimum solution for every combination of desired and unwanted signals due to the limitation on the number of the predefined beams.

An advantage of switched beamforming over the adaptive one is its fast response to changes in the electromagnetic environment. On the other hand, in contrary to switched beamforming, adaptive beamforming can achieve the optimum solution for all possible combination of the target signals.

In this thesis, we propose a novel multi-model approach that combines the advantages of the switched and adaptive beamforming techniques inspired from [7]. The proposed *Multi-Model Adaptive Approach* combines a switched beamforming system with an adaptive beamforming system.

5.1. Multi-Model Beamformer

The architecture of the proposed multi-model beamformer is depicted in Fig. 5.1. It consists of a bank of fixed beamformers, an adaptive beamformer and an adaptive beamformer whose parameters are initialized every time there is a sudden change in the received signal(s). Details of the sub-blocks and the structure of the proposed system are studied in the following subsections.
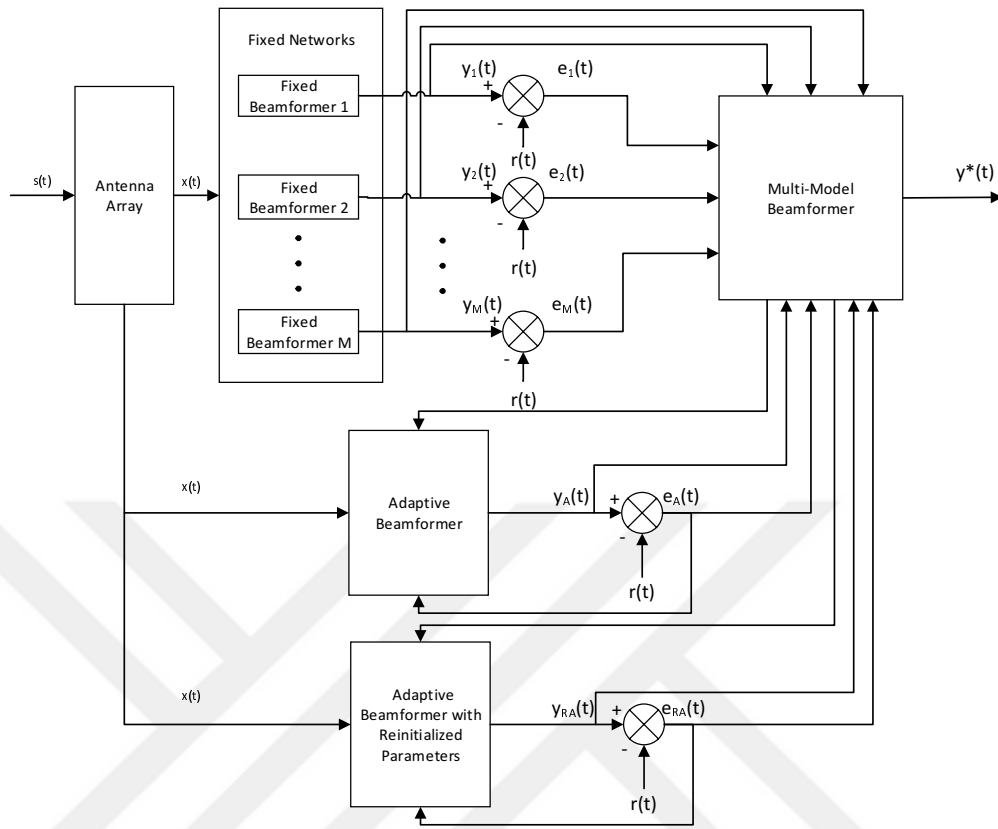
Figure 5.1. General Architecture of Switched Adaptive with One Reinitialized
Adaptive System

In order to compare the performance of the proposed multi-model beamformer
with a classical adaptive system, we carry out simulations in Matlab. For simplicity,
the MSE method is used to create multi-beams of the switched beamforming and the
LMS method is used as adaptive beamforming method. There are 5° between each
beam used in switched beamforming. The direction of the desired signal is chosen as
2° because switched beamforming system has maximums at the multitude of 5°s and
the interferer signal comes from $-25°$. At 100th time interval, desired signal changes
and the new desired signal comes from 32°. Thus, we can also observe the performances
of the defined systems for both, stable and suddenly changing DOA of the signals.

Figure 5.2. General Architecture of M Fixed Beamforming Models and Controller
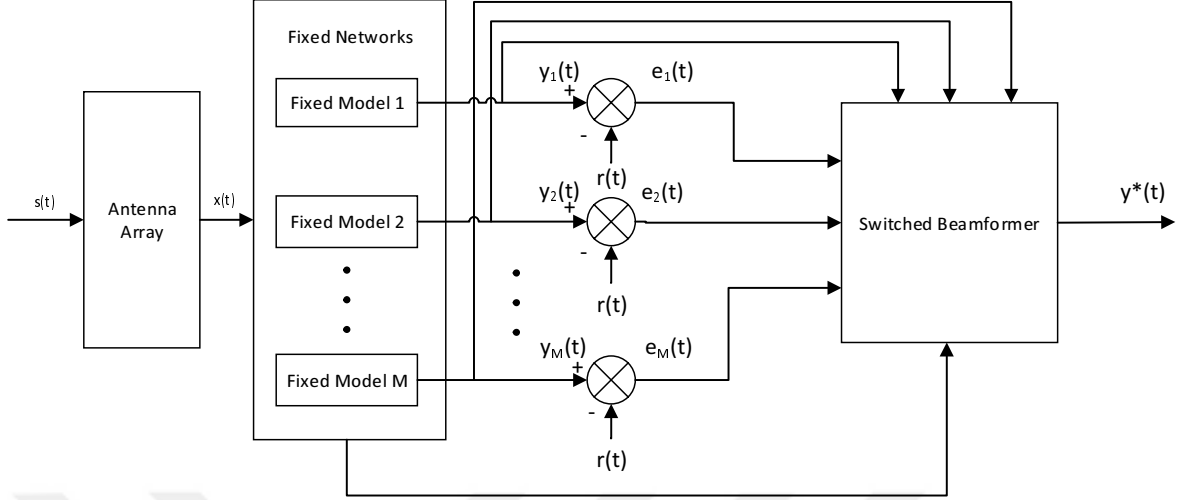
5.1.1. Fixed Beamformer

Figure 5.2 shows the general architecture of a switched beamforming system using M fixed beamforming networks and a controller. All fixed beamforming networks are fed by antenna array outputs. The outputs of these networks are compared to the reference signal $r(t)$. The controller gets the error outputs $e_i(t)$, and chooses the best fixed beamforming network which results in minimum error. Therefore, the system output $y^*(t)$ is actually one of the fixed beamforming networks' outputs $y_1(t), y_2(t)..., y_M(t)$ which produces the minimum error.

The output of each fixed beamformer is computed as

$$y_i(t) \;=\; w_{Fi}^H x(t), \quad e_i(t) \;=\; r(t) - y_i(t), \quad i = 1, 2, ...M \tag{5.1}$$

where M is the number of the fixed beamformer networks, w_{Fi} is antenna weight of the ith fixed network, $e_i(t)$ is error of ith fixed beamformer output and $r(t)$ is the reference signal.

To evaluate the performance of the switched beamformer, consider a Switched
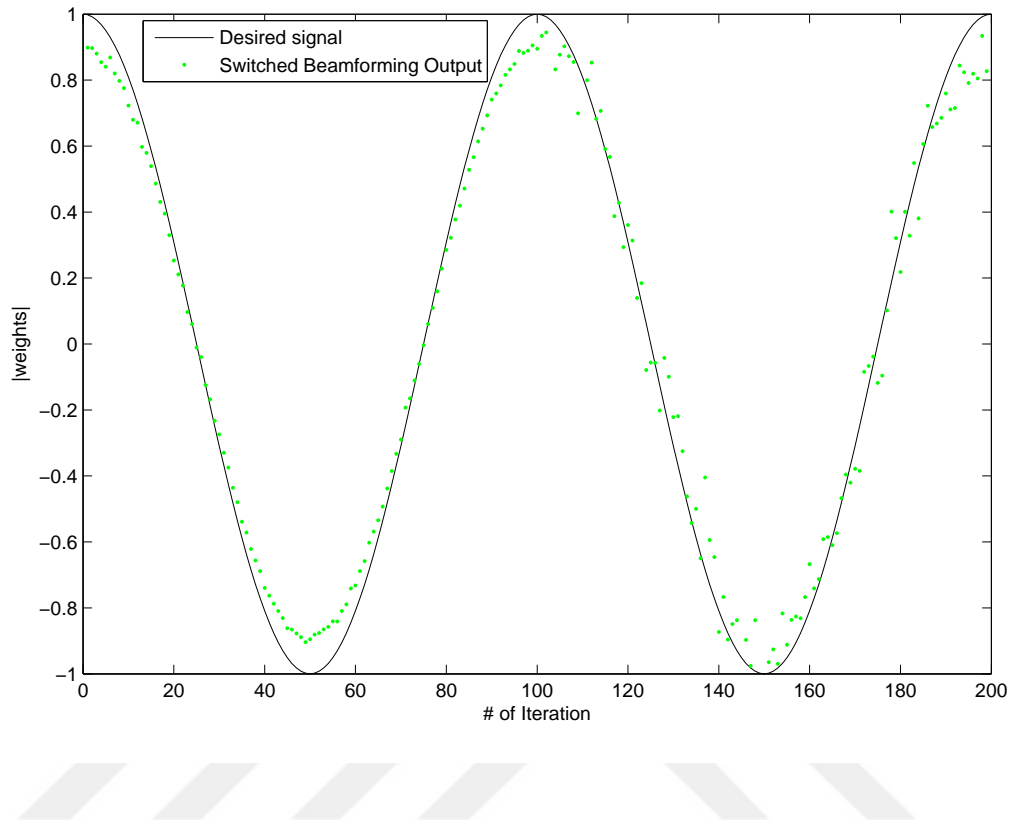
Figure 5.3. Output of the Switched Beamforming System

Beamforming System that consists of fixed beams with 5° separation. The output of
the Switched Beamforming System to the signals defined in Sec. 5.1 is shown in Fig.
5.3. Since the system does not have ideal solutions for all SOIs and SNOIs, the output
never converges to the desired signal. It chooses the best fixed beam that conforms
the signals, and results in a constant error that is same for every period of the signal.
System rapidly changes the beam to the best conforming one to the new signals defined
at the $100th$ time interval.

5.1.2. Adaptive Beamformer

Although fixed beamforming methods with switched beamforming provide a so-
lution to direction changes of the incoming signals, it may not be the optimum solution
due to impossibility of covering all possible SOI and SNOI directions. It can be easily
seen from Fig. 4.7 that it is not the optimum solution for the signals in the figure. Not

Figure 5.4. General Architecture of Adaptive Beamforming System
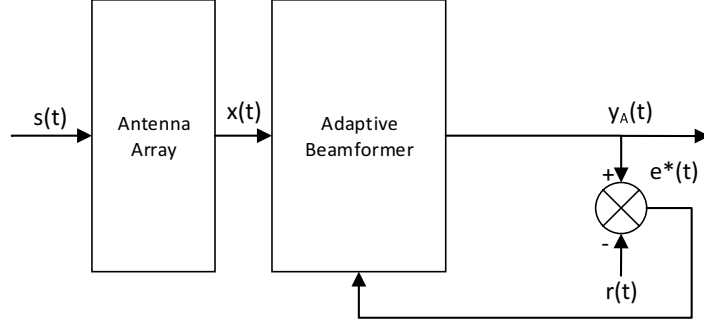
only the SNOIs are not arrived at the *null* directions but also the main beam is not at the absolute direction of the SOI. Thus, SNOIs cannot be cancelled and will affect the SOI negatively as noise in the output of the beamforming network.

Adaptive beamforming methods are used to solve the problem with the signals whose directions change in time. Adaptive beamforming systems have a feedback network and try to adopt themselves to new conditions in the electromagnetic environment. Fig 5.4 is a representation of the general architecture of Adaptive Beamforming System. The antenna weight vector w_A which is updated with time and the output of adaptive beamformer y_A are computed as follows

$$w_A^H(k) = w_A^H(k-1) + \mu e_A(k)x(k-1) \tag{5.2}$$

$$y_A(k) = w_A^H(k)x(k), \quad e_A(k) = r(k) - y_A(k) \tag{5.3}$$

where μ is the forgetting factor, e_A is error of the adaptive beamformer output, r is the reference signal.

The array output of the *Adaptive Beamforming System* created by using LMS method to the signals defined in Sec. 5.1 is shown in Fig 5.5. The convergence of the output of the system to the desired signal takes approximately 70 time intervals, after which the system perfectly matches the desired output until a change in the direction of the SOI and SNOI. At $100th$ time interval, sudden change of the direction of the SOI
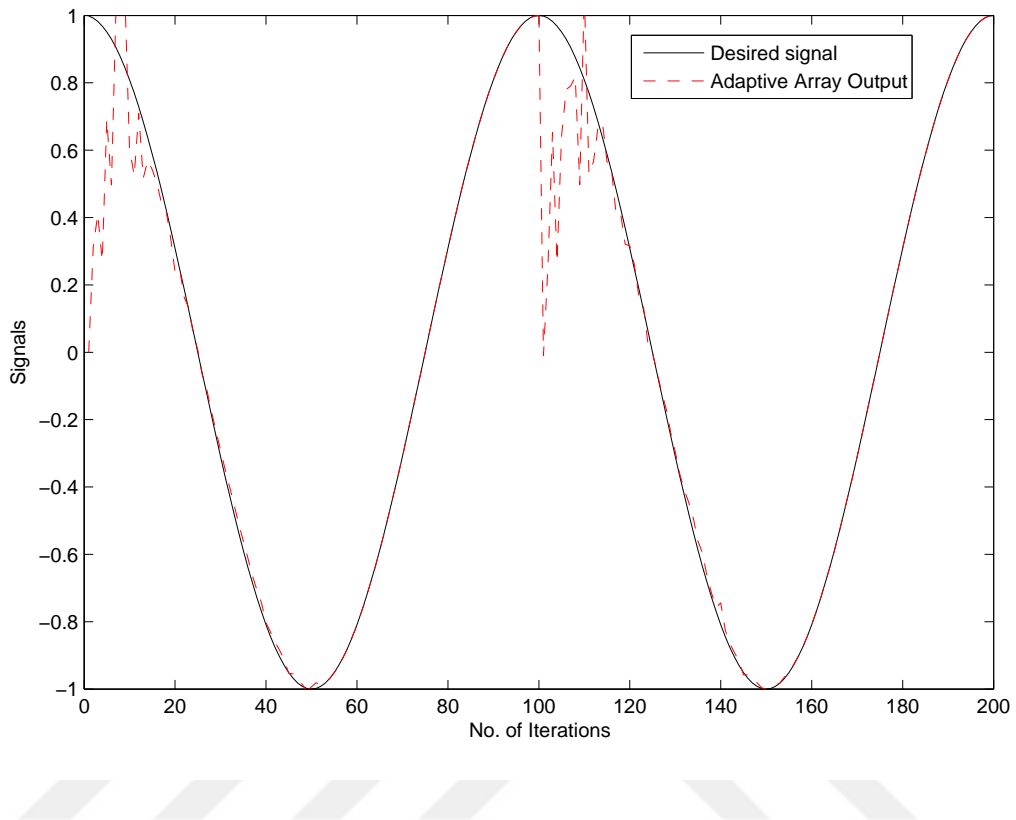
Figure 5.5. Output of the Adaptive Beamforming System

from 2° to 32° results in huge errors in the Adaptive Beamforming System output. It takes a new approximately 70 time intervals for convergence of the output of the system to the desired signal. Along these lines, we can conclude that despite the Adaptive Beamforming System has huge errors in sudden direction changes of the SOI and/or SNOI, its output perfectly converges to the desired signal eventually.

5.1.3. Switched Adaptive Beamformer

Switched Adaptive Beamforming model is the combination of a Switched and Adaptive Beamforming models with a controller. Since the controller is fed by the outputs of a Switched Beamforming System and an Adaptive Beamforming System and decides the best option, it is referred to as a *Multi Model* system. The Switched Adaptive System takes snapshots and calculates the error at each instance. The system itself decides how the system response should be for optimum performance. If

there is no sudden change, meaning small error, it behaves as an adaptive system. If there is a sudden change in the signals, it chooses the optimum fixed beamforming network from the switched beamforming system and equates the adaptive beamforming antenna weights to this fixed network's antenna weights. Therefore, the system gives rapid response to sudden changes in the target directions as a switched beamforming system, and achieves optimum solution for each different combination of the desired and unwanted signals as an adaptive beamforming system.

The output of only switched adaptive beamformer is computed as

$$y^*(t) = \begin{cases} y_A(t) & if \ \ e_A(t) < e_F(t) \\ y_F(t) & else \end{cases}$$

where w_A is antenna weight vector of the adaptive network which is updated with time.

The array output of the *Switched Adaptive Beamforming System* to the signals defined in Sec. 5.1 is shown in Fig 5.6. The convergence of the output of the system to the desired signal takes approximately $20 - 25$ time intervals. Afterwards, the system perfectly matches the desired output like an adaptive system until a change in the direction of the SOI and SNOI. At the $100th$ time interval, a sudden change of the direction of the SOI from $2°$ to $32°$ results in small errors in the Switched Adaptive Beamforming System output in contrast to Adaptive Beamforming System. It takes another $20 - 25$ time intervals to convergence. Hence, we can conclude that despite the Adaptive Beamforming System has huge errors in sudden direction changes of the SOI and/or SNOI, its output perfectly converges to the desired signal in a short amount of time.

5.1.4. Switched Adaptive with One Reinitialized Adaptive Beamformer

Switched Adaptive Model with One Reinitialized Adaptive Model contains one more Adaptive Beamforming System whose antenna weights are zeroed at time instants when switching the beamforming system from adaptive to fixed one occurs. It works
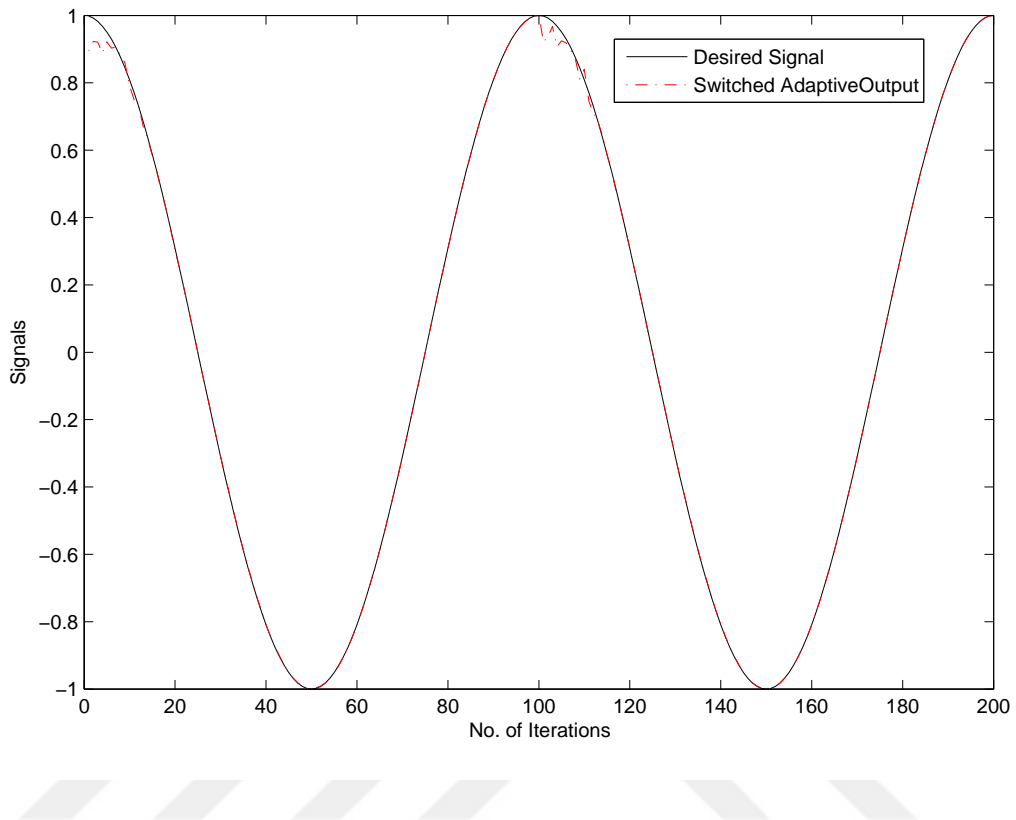
Figure 5.6. Array Outputs of Switched Adaptive Beamforming

similar to a *Switched Adaptive System*. The system itself decides how the system response should be for optimum performance. If there is no sudden change, meaning small error, it behaves as an adaptive system. If there is a sudden change in the signals, it chooses the optimum fixed beamforming network from the switched beamforming system and equates one of the adaptive beamforming antenna weights to this fixed network's antenna weights and zeroes the other adaptive beamforming antenna weights. Therefore, the system gives fast response to sudden changes in the target directions as a switched beamforming system, and achieves optimum solution for each different combination of the desired and unwanted signals as an adaptive beamforming system.

Reinitialization of antenna weights is proposed in [8, 47, 48] to overwhelm the situation that adaptive system favors to track the stronger interference signal if the moving SOI is weak and gets in spatial coherency with a stronger interference signal. In our case, we use reinitialization of antenna weights to obtain optimum beam pattern.
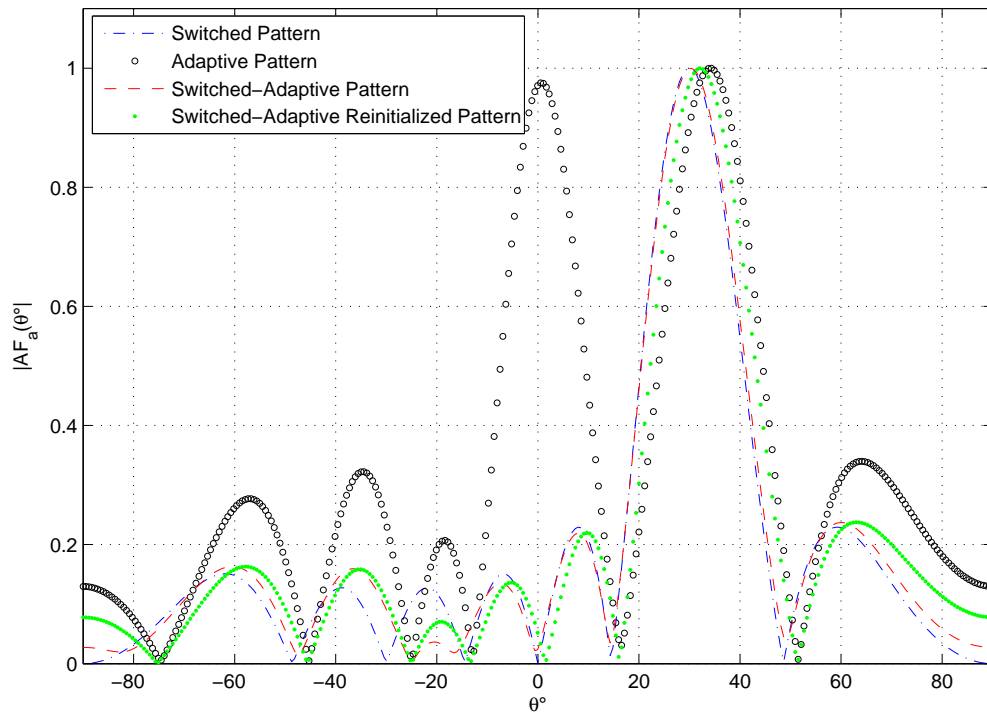
Figure 5.7. Final Beam Patterns of Switched, Adaptive and Switched Adaptive
Beamforming Systems

Adaptive Model cannot perfectly remove the main beam that corresponds to the former direction of the SOI due to the no signal in that direction after the change of the direction of the SOI. Reinitialized Adaptive Model removes this beam and prevents the system to be affected from the temporary signals in this direction.

Figs. 5.7-5.8 show the final beam patterns of *Only Multiple-Fixed, Only Adaptive, Switched Adaptive and Switched Adaptive with One Reinitialized Adaptive* beamforming systems. At the beginning, SOI comes from $2°$ and SNOI comes from $-25°$. At 100th time interval, direction of the SOI changes to $32°$ and SNOI remains in the same direction. As seen from the figure, *Switched Beamforming System* cannot match the SOI and SNOI bearings perfectly. *Adaptive Beamforming System* can match the SOI and SNOI bearings but it cannot remove the main beam that corresponds to the former direction of the SOI due to the no signal in that direction after the change
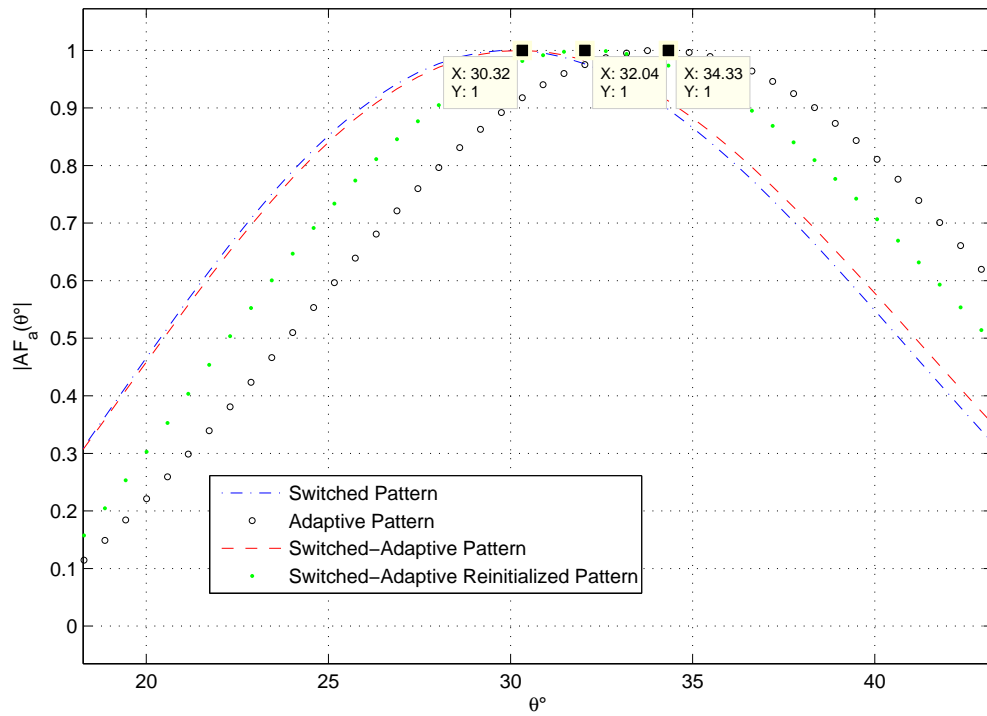
Figure 5.8. Final Beam Patterns of Switched, Adaptive and Switched Adaptive
Beamforming Systems

of the direction of the SOI. In addition, Adaptive Beamforming System's main beam points to $32°$ whereas the SOI is at $34°$. In spite of the fact that *Switched Adaptive System* gives better results than Switched and Adaptive systems, its main beam also points with a $2°$ error. Since it jumps to the optimum fixed beamforming network whose main beam is at $30°$ direction, it does not change with time due to small angle difference between SOI and the main beam of the fixed network. *Switched Adaptive with One Reinitialized Adaptive Beamforming System* gives the best result for all criteria. The main beam is in the correct direction, SNOI is cancelled perfectly and there is no second main beam as in the Adaptive Beamformer. It combines the nice characteristics of Switched, Adaptive and Switched Adaptive models and does not suffer from their problems.

Fig. 5.9 shows the array outputs of Switched, Adaptive and Switched Adaptive
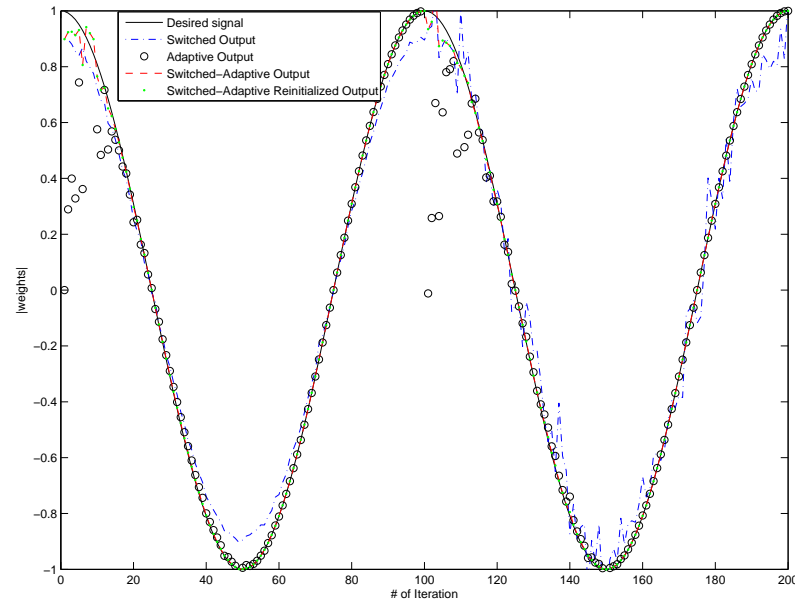
Figure 5.9. Array Outputs of Switched, Adaptive and Switched Adaptive
Beamforming Systems

Beamforming Systems. Multi-Model adaptive beamforming systems decrease the error faster than classical adaptive beamforming system. After $20 - 25$ iterations, it yields results approximately with zero error. On the other hand, for the same performance, adaptive beamforming system requires $65 - 70$ iterations. In addition, single adaptive beamforming system gives huge errors when sudden changes occur in the direction of the SOI. Since switched beamforming system cannot match the SOI and SNOI perfectly, it results in continuous errors in the output.

It can be easily seen from Fig. 5.10 that multi-model adaptive beamforming systems' weights converge faster than classical adaptive beamforming system. It converges in $20 - 25$ iterations, whereas the convergence of adaptive beamforming system is in $55 - 60$ iterations. Switched Adaptive Beamforming system takes the advantage of choosing approximately true weights for initial antenna weights, thus perform better results than adaptive method. The antenna weights of the Switched Adaptive Beamforming with One Reinitialized Adaptive Beamforming System are the same with the
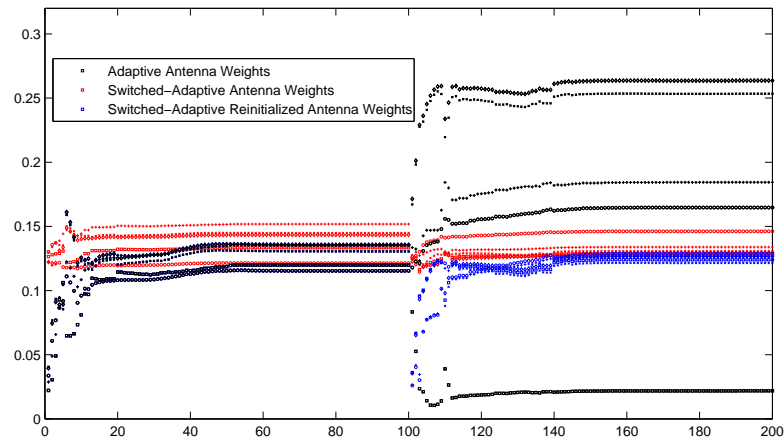
Figure 5.10. Antenna Weights of Adaptive and Switched Adaptive Beamforming Systems

Adaptive Beamforming System's antenna weights at the beginning. After the sudden change of the SOI direction, antenna weights of the Switched Adaptive Beamforming with One Reinitialized Adaptive Beamforming System are zeroed and separated from Adaptive Beamforming System's antenna weights.

Mean square errors of the Switched Adaptive Beamforming Systems are smaller than mean square errors of the Switched and Adaptive Systems. Fig. 5.11 shows the comparison of mean square errors of all systems. Switched Beamforming System results in continuous errors in the output. Adaptive Beamforming System gives huge errors in the sudden direction changes of the SOI and SNOI. Compared to other systems, Switched Adaptive Beamforming Systems start with small errors and converge to zero error in a short time.

5.2. Summary of the Chapter & Concluding Remarks

In this chapter, we have proposed a novel multi-model beamformer inspired from Narendra [7] that integrates the switched and adaptive beamforming systems. The proposed multi-model adaptive beamforming system enjoys the advantages of both

Figure 5.11. MSE of Switched, Adaptive and Switched Adaptive Beamforming Systems

switched and adaptive beamforming. It does not add too much computational complexity to an adaptive only beamforming system, due to the simple calculations of the switched beamforming system. It gives faster response than an adaptive only system and it provides perfect tracking to all possible combinations of desired signal and unwanted signals as opposed to a switched beamforming system.

6. CONCLUSIONS

In the first part of the thesis, we have implemented an FFT based Correlative Interferometer Method for different antenna apertures and have evaluated system performance as a function of antenna aperture d. Simulation studies have been carried out to confirm that RMS error of the system decreases with increasing antenna aperture. On the other hand, for antenna aperture d greater than half of the input signal wavelength, there is an ambiguity on the actual AOA.

To resolve the ambiguity resulting from the antenna aperture greater than half of the incoming signal wavelength by using FFT based Correlative Interferometer Method, we have studied the effect of increasing the number of non-parallel baselines (antenna pairs) in the system. We have verified that increasing non-parallel baselines can overcome this ambiguity, while increasing the number of antenna elements alone may not be sufficient. More specifically, one can deduce that using antenna elements at prime numbers has more power to solve this ambiguity, e.g., use 5 antenna rather than 4, 6 or 8 antennas; use 7 antennas rather than 6, 8 or 12 antennas. Another conclusion we can draw from our simulation analysis is that increasing the number of the antenna elements in the system provides more accurate results.

In the second part of the thesis, we focus on *Smart Antennas*. Firstly, beamforming approaches used in Smart Antennas have been discussed in detail. We review that an advantage of switched beamforming over the adaptive one is its fast response to changes in the electromagnetic environment. On the other hand, in contrast to switched beamforming, adaptive beamforming can achieve close to perfect tracking for all possible combination of target signals.

One of the main contributions of this thesis has been to propose a multi-model beamformer inspired from [7] that integrates the switched and adaptive beamforming systems. The proposed multi-model adaptive beamforming system enjoys the advantages of both switched and adaptive beamforming while it does not add too much
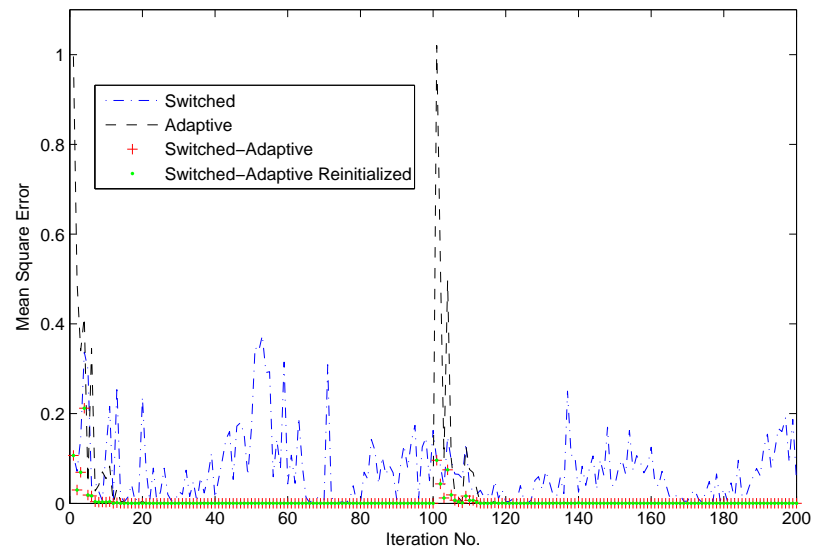
computational complexity to an adaptive only beamforming system, due to the simple calculations of the switched beamforming system. It provides faster response than an adaptive only system and it achieves perfect tracking for all possible combinations of desired and unwanted signals contrary to a switched beamforming only system.

REFERENCES

1. Kebeli, M., "Extended symmetrical aperture direction finding using correlative interferometer method", *Electrical and Electronics Engineering (ELECO), 2011 7th International Conference on*, pp. II–209 –II–213, Dec 2011.

2. Lipsky, S. E., *Microwave Passive Direction Finding*, SciTech Publishing, Inc., Raleigh, NC 27613, USA, 2004.

3. Jenkins, H. H., *Small-Aperture Radio Direction Finding*, Artech House, Inc., Norwood, MA 02062, USA, 1991.

4. Travers, N. D. and S. M. Hixon, "Abstracts of the Available Literature on Radio Direction Finding 1899-1965", Technical report, DTIC Document, 1966.

5. Boyd, J. A., D. B. Harris, U. of Michigan Institute of Science & Technology, D. D. King, and H. W. Welch, *Electronic Countermeasures*, Defense Technical Information Center, 1961.

6. Rohde-Schwarz, *Introduction into Theory of Direction Finding*, 2004, `http://www.rohde&schwarz.com`, Jan 2009.

7. Narendra, K. and J. Balakrishnan, "Adaptive Control Using Multiple Models", *Automatic Control, IEEE Transactions on*, Vol. 42, No. 2, pp. 171–187, Feb 1997.

8. George, K., "Some Applications of Multiple Models Methodology", *15th Yale Workshop on Adaptive and Learning Systems*, pp. 81–86, Yale University, New Haven, CT, USA, June 2011.

9. Products, R., *A User's Guide To Radio Direction Finding Basics*, 1998, `http://www.rdfproducts.com/wn001_apl_01.pdf`, July 2009.

10. Gething, P. J. D., *Radio Direction Finding and the Resolution of Multicomponent Wave-Fields*, Peter Peregrunus Ltd., London, UK, 1986.

11. Cianos, N., "The New Generation of Direction Finding and Intercept Systems", *Journal of Electronic Defense*, Oct 1992.

12. Lipsky, S. E., "Find the Emitter Fast with Monopulse Methods", *Microwave*, May. 1978.

13. Foutz, J., A. Spanias, and M. K. Banavar, *Narrowband Direction of Arrival Estimation for Antenna Arrays*, Morgan & Claypool, 2008.

14. Adcock, F., *"Improvement in Means for Determining the Direction of a Distant Source of Electromagnetic Radiation"*, British Patent 1304901919, 1917.

15. Baghdady, E. J., "New developments in direction-of-arrival measurement based on Adcock antenna clusters", *Aerospace and Electronics Conference, 1989. NAECON 1989., Proceedings of the IEEE 1989 National*, pp. 1873–1879 vol.4, May 1989.

16. Products, R., *A Comparison Of The Watson-Watt And Pseudo-Doppler DF Techniques*, 1998, `http://www.rdfproducts.com/wn004_apl_01.pdf`, july 2009.

17. KØOV, J. M., *RDF FAQ*, 1995, `http://members.aol.com/homingin/FAQ.html`, may 2008.

18. Instruments, D. D., *Doppler Pulse Principles*, 1999, `http://www.silcom.com/~{}pelican2/PicoDopp/MORE_PULSES.html`, July 2009.

19. Cianos, N., "Low-cost, high-performance DF and intercept systems", *WESCON/'93. Conference Record,*, pp. 372–376, Sep 1993.

20. Peavey, D. and T. Ogumfunmi, "The single channel interferometer using a pseudo-Doppler direction finding system", *Acoustics, Speech, and Signal Processing, 1997. ICASSP-97., 1997 IEEE International Conference on*, Vol. 5, pp. 4129–4132, Apr

1997.

21. Godara, L., "Application of Antenna Arrays to Mobile Communications, Part II: Beam-Forming and Direction-of-Arrival Considerations", *Proceedings of the IEEE*, Vol. 85, No. 8, pp. 1195–1245, 1997.

22. Stoica, P. and R. Moses, *Introduction to Spectral Analysis*, Prentice Hall, Upper Saddle River, NJ, 1997.

23. Mayhan, J. and L. Niro, "Spatial spectral estimation using multiple beam antennas", *IEEE Transactions on Antennas and Propagation*, Vol. 35, No. 8, pp. 897–906, Apr. 1987.

24. Capon, J., "High resolution frequency-wavenumber spectral analysis", *Proceedings of the IEEE*, Vol. 57, p. 1408–1518, Aug. 1969.

25. Schmidt, R., "Multiple emitter location and signal parameter estimation", *Antennas and Propagation, IEEE Transactions on*, Vol. 34, No. 3, pp. 276–280, 1986.

26. Zoltowski, M. D., G. M. Kautz, and S. Silverstein, "Beamspace ROOT-MUSIC", *IEEE Transactions on Antennas and Propagation*, Vol. 41, No. 1, pp. 344–364, Feb. 1993.

27. Xu, G., S. Silverstein, R. Roy, and T. Kailath, "Beamspace ESPRIT", *IEEE Transactions on Signal Processing*, Vol. 42, No. 2, pp. 349–356, Feb. 1994.

28. Swindlehurst, A., B. Ottersten, R. Roy, and T. Kailath, "Multiple invariance ESPRIT", *Signal Processing, IEEE Transactions on*, Vol. 40, No. 4, pp. 867–881, Apr 1992.

29. Haardt, M. and J. A. Nossek, "Unitary ESPRIT: how to obtain increased estimation accuracy with a reduced computational burden", *IEEE Transactions on Signal Processing*, Vol. 43, No. 2, pp. 1232–1242, May. 1995.

30. Wu, Y.-W., S. Rhodes, and E. Satorius, "Direction of arrival estimation via extended phase interferometry", *Aerospace and Electronic Systems, IEEE Transactions on*, Vol. 31, No. 1, pp. 375–381, Jan 1995.

31. Jacobs, E. and E. Ralston, "Ambiguity Resolution in Interferometry", *Aerospace and Electronic Systems, IEEE Transactions on*, Vol. AES-17, No. 6, pp. 766–780, Nov 1981.

32. King, N. R., M. P. Baker, I. W. N. Pawson, R. N. Shaddock, and E. J. Stansfield, "Direction Finding", 1984.

33. Balanis, C. A., *Antenna Theory: Analysis and Design*, Wiley-Interscience, New York, 2005.

34. Kraus, J. and R. Marhefka, *Antennas for All Applications (3rd Ed.)*, McGraw-Hill, New York, 2002.

35. Liberti, J. C. and T. S. Rappaport, *Smart Antennas for Wireless Communications: IS-95 and Third Generation CDMA Applications*, Prentice-Hall, Inc., New Jersey, 1997.

36. Stutzman, W. and G. Thiele, *Antenna Theory and Design*, Wiley, New York, 1981.

37. Johnson, D. and D. Dudgeon, *Array Signal Processing—Concepts and Techniques*, Prentice-Hall, Inc., New Jersey, 1993.

38. Monzingo, R. and T. Miller, *Introduction to Adaptive Arrays*, Wiley, New York, 1980.

39. Butler, J. and R. Lowe, "Beam-Forming Matrix Simplifies Design of Electrically Scanned Antennas", *Electronic Design*, Apr. 1961.

40. Gross, F., *Smart antennas for wireless communications: with MATLAB*, Professional engineering, McGraw-Hill, 2005.

41. Litva, J. and T. K. Lo, *Digital Beamforming in Wireless Communications*, Artech House, Inc., Norwood, MA, USA, 1st edition, 1996.

42. Van Trees, H., *Detection, Estimation, and Modulation Theory*, number 1. böl. in Detection, Estimation, and Modulation Theory, Wiley, 2004.

43. Van Trees, H., *Detection, Estimation, and Modulation Theory: Optimum array processing*, Detection, Estimation, and Modulation Theory, Wiley, 1968.

44. Haykin, S., *Adaptive Filter Theory (4th Ed.)*, Prentice Hall, New York, USA, 2002.

45. Burg, J. P., "The Relationship Between Maximum Entropy Spectra and Maximum Likelihood Spectra", *Geophysics*, Vol. 37, No. 2, pp. 375–376, 1972.

46. Golub, G. H. and C. F. Van Loan, *Matrix Computations (3rd Ed.)*, The Johns Hopkins University Press, Baltimore, MD, USA, 1996.

47. George, K. and K. S. Sajjanshetty, "On the Blind Separation of Signals from Moving Sources Using Switching and Tuning", *Computational Intelligence, Modelling and Simulation, International Conference on*, Vol. 0, pp. 299–304, 2010.

48. George, K. and K. Sajjanshetty, "On the reception of a moving signal despite moving interferences", *Industrial and Information Systems (ICIIS), 2010 International Conference on*, pp. 125–130, July 2010.